

Title Page

Supplemental Table S1: Sensory processing in humans and mice fluctuates between external and internal modes

Authors:

Veith Weilnhammer^{1,2,3}, Heiner Stuke^{1,2}, Kai Standvoss¹, Philipp Sterzer⁴

Affiliations:

¹ Department of Psychiatry, Charité-Universitätsmedizin Berlin, corporate member of Freie Universität Berlin and Humboldt-Universität zu Berlin, 10117 Berlin, Germany

² Berlin Institute of Health, Charité-Universitätsmedizin Berlin and Max Delbrück Center, 10178 Berlin, Germany

³ Helen Wills Neuroscience Institute, University of California Berkeley, USA

⁴ Department of Psychiatry (UPK), University of Basel, Switzerland

Corresponding Author:

Veith Weilnhammer, Helen Wills Neuroscience Institute, University of California Berkeley, USA, email: veith.weilnhammer@gmail.com

¹ **1 Supplemental Table S1**

² **1.1 Internal mode processing is driven by choice history as opposed
3 to stimulus history**

⁴ The main manuscript reports the effects of perceptual history, which we defined as the impact
⁵ of the choice at the preceding trial on the choice at the current trial (henceforth *choice*
⁶ *history*). *Stimulus history*, which is defined as the impact of the stimulus presented at the
⁷ preceding trial on the choice at the present trial, represents an alternative approach to this.
⁸ Here, we compare the effects of choice history to the effects of stimulus history.

⁹ We observed a significant bias toward stimulus history (humans: $49.76\% \pm 0.1\%$ of trials, β
¹⁰ $= 1.26 \pm 0.94$, $T(373.62) = 1.34$, $p = 0.18$; mice: $51.11\% \pm 0.08\%$ of trials, $T(164) = 13.4$, p
¹¹ $= 3.86 \times 10^{-28}$). The bias toward stimulus history was smaller than the bias toward choice
¹² history (humans: $\beta = -3.53 \pm 0.5$, $T(66.53) = -7.01$, $p = 1.48 \times 10^{-9}$; mice: $T(164) =$
¹³ -17.21 , $p = 1.43 \times 10^{-38}$).

¹⁴ The attraction of choices toward both preceding choices and stimuli is expected, as perception
¹⁵ was *stimulus-congruent* on approximately 75% of trials, causing choices and stimuli to be
¹⁶ highly correlated. We therefore compared the effects of choice history and stimulus history
¹⁷ after *stimulus-incongruent* (i.e., *error*) trials, since those trials lead to opposite predictions
¹⁸ regarding the perceptual choice at the subsequent trial.

¹⁹ As expected from the findings presented in the main manuscript, perceptual choices were
²⁰ attracted toward perceptual choices when the inducing trial was stimulus-incongruent (i.e., a
²¹ positive effect of choice history; humans: $\beta = 0.19 \pm 1.4 \times 10^{-4}$, $z = 1.36 \times 10^3$, $p < 2.2 \times 10^{-308}$:
²² mice: $\beta = 0.92 \pm 0.01$, $z = 88.82$, $p < 2.2 \times 10^{-308}$). By contrast, perceptual choices tended
²³ to be repelled away from the stimulus presented at preceding stimulus-incongruent trial
²⁴ (i.e., a negative effect of stimulus history; humans: $\beta = -0.19 \pm 0.01$, $z = -16.47$, $p =$
²⁵ 5.99×10^{-61} : mice: $\beta = -0.92 \pm 0.01$, $z = -88.76$, $p < 2.2 \times 10^{-308}$). This repulsion of

26 choices away from stimuli presented at stimulus-incongruent trials confirmed that choices
27 (which are anti-correlated to stimuli at stimulus-incongruent trials) were the primary driver
28 of attracting serial effects in perception.

29 In sum, the above results suggest that, in both humans and mice, serial dependencies were
30 better explained by the effects of choice history as opposed to the effects of stimulus history.
31 This aligns with a result recently published for the IBL database, where mice were shown to
32 follow an *action-kernel* as opposed to a *stimulus-kernel* model when integrating information
33 across trials⁸¹.

34 **1.2 Fluctuations between internal and external mode modulate
35 perceptual performance beyond the effect of general response
36 biases**

37 The hypothesis that perception cycles through opposing internally- and externally-biased
38 modes is motivated by the assumption that recurring intervals of stronger perceptual history
39 temporally reduce the participants' sensitivity to external information. Importantly, the
40 history-dependent biases that characterize internal mode processing must be differentiated
41 from general response biases. In binary perceptual decision-making, general response biases
42 are defined by a propensity to choose one of the two outcomes more often than the alternative.
43 Indeed, human participants selected the more frequent of the two possible outcomes in 58.71%
44 \pm 0.22% of trials, and mice selected the more frequent of the two possible outcomes in 54.6%
45 \pm 0.3% of trials.

46 Two caveats have to be considered to make sure that the effect of history-congruence is
47 distinct from the effect of general response biases. First, history-congruent states become
48 more likely for larger response biases that cause an increasing imbalance in the likelihood of
49 the two outcomes (humans: $\beta = 0.24 \pm 6.93 \times 10^{-4}$, $T(2.09 \times 10^6) = 342.43$, $p < 2.2 \times 10^{-308}$;
50 mice: $\beta = 0.15 \pm 8.25 \times 10^{-4}$, $T(1.32 \times 10^6) = 181.93$, $p < 2.2 \times 10^{-308}$). One may thus

51 ask whether the autocorrelation of history-congruence could be entirely driven by general
52 response biases.

53 Importantly, our autocorrelation analyses account for general response biases by computing
54 group-level autocorrelations (Figure 2-4B) relative to randomly permuted data (i.e., by
55 subtracting the autocorrelation of randomly permuted data from the raw autocorrelation
56 curve). This precludes that general response biases contribute to the observed autocorrelation
57 of history-congruence (see Supplemental Figure S5 for a visualization of the correction
58 procedure for simulated data with general response biases ranging from 60 to 90%).

59 Second, it may be argued that fluctuations in perceptual performance may be solely driven
60 by ongoing changes in the strength of general response biases. To assess the links between
61 dynamic fluctuations in stimulus-congruence on the one hand and history-congruence as well
62 as general response bias on the other hand, we computed all variables as dynamic probabilities
63 in sliding windows of ± 5 trials (Figure 1C). Linear mixed effects modeling indicated that
64 fluctuations in history-congruent biases were larger in amplitude than the corresponding
65 fluctuations in general response biases in humans ($\beta_0 = 0.03 \pm 7.34 \times 10^{-3}$, $T(64.94) = 4.46$,
66 $p = 3.28 \times 10^{-5}$), but slightly smaller in mice ($\beta_0 = -5.26 \times 10^{-3} \pm 4.67 \times 10^{-4}$, $T(2.12 \times 10^3)$
67 $= -11.28$, $p = 1.02 \times 10^{-28}$).

68 Crucially, ongoing fluctuations in history-congruence had a significant negative effect on
69 stimulus-congruence (humans: $\beta_1 = -0.05 \pm 5.63 \times 10^{-4}$, $T(2.1 \times 10^6) = -84.21$, $p <$
70 2.2×10^{-308} ; mice: $\beta_1 = -0.12 \pm 7.17 \times 10^{-4}$, $T(1.34 \times 10^6) = -168.39$, $p < 2.2 \times 10^{-308}$)
71 beyond the effect of ongoing changes in general response biases (humans: $\beta_2 = -0.06 \pm$
72 5.82×10^{-4} , $T(2.1 \times 10^6) = -103.51$, $p < 2.2 \times 10^{-308}$; mice: $\beta_2 = -0.03 \pm 6.94 \times 10^{-4}$,
73 $T(1.34 \times 10^6) = -48.14$, $p < 2.2 \times 10^{-308}$). In sum, the above control analyses confirmed
74 that, in both humans and mice, the observed influence of preceding choices on perceptual
75 decision-making cannot be reduced to general response biases.

76 **1.3 Internal mode is characterized by lower thresholds as well as**
77 **by history-dependent changes in biases and lapses**

78 Random or stereotypical responses may provide an alternative explanation for the reduced
79 sensitivity to external sensory information that we attribute to internal mode processing. To
80 test this hypothesis, we asked whether history-independent changes in biases and lapses may
81 provide an alternative explanation of the reduced sensitivity during internal mode.

82 To this end, we estimated full and history-conditioned psychometric curves to investigate how
83 internal and external mode relate to biases (i.e., the horizontal position of the psychometric
84 curve), lapses (i.e., the asymptotes of the psychometric curve) and thresholds (i.e., 1/sensitivity,
85 estimated from the slope of the psychometric curve). We used a maximum likelihood procedure
86 to predict trial-wise choices y ($y = 0$ and $y = 1$ for outcomes A and B respectively) from
87 the choice probabilities y_p . y_p was computed from the difficulty-weighted inputs s_w via a
88 parametric error function defined by the parameters γ (lower lapse), δ (upper lapse), μ (bias)
89 and t (threshold; see Methods for details):

$$y_p = \gamma + (1 - \gamma - \delta) * (\text{erf}\left(\frac{s_w + \mu}{t}\right) + 1)/2 \quad (1)$$

90 Under our main hypothesis that periodic reductions in sensitivity to external information
91 are driven by increases in the impact of perceptual history, one would expect (i) a history-
92 dependent increase in biases and lapses (effects of perceptual history), and (ii), a history-
93 independent increase in threshold (reduced sensitivity to external information). Conversely,
94 if what we identified as internal mode processing was in fact driven by random choices, one
95 would expect (i), a history-independent increase in lapses (choice randomness), (ii), no change
96 in bias (no effect of perceptual history), and (iii), reduced thresholds (reduced sensitivity to
97 external information).

98 **1.3.1 Humans**

99 Across all data provided by the Confidence database²⁰ (i.e., irrespective of the preceding
100 perceptual choice y_{t-1}), biases μ were distributed around zero (-0.05 ± 0.03 ; $\beta_0 = 7.37 \times 10^{-3}$
101 ± 0.09 , $T(36.8) = 0.08$, $p = 0.94$; Supplemental Figure 6A-B, upper panel). When conditioned
102 on perceptual history, biases μ varied according to the preceding perceptual choice, with
103 negative biases for $y_{t-1} = 0$ (-0.22 ± 0.04 ; $\beta_0 = 0.56 \pm 0.12$, $T(43.39) = 4.6$, $p = 3.64 \times 10^{-5}$;
104 Supplemental Figure 6A-B, upper panel) and positive biases for $y_{t-1} = 1$ (0.29 ± 0.03 ; β_0
105 $= 0.56 \pm 0.12$, $T(43.39) = 4.6$, $p = 3.64 \times 10^{-5}$; Supplemental Figure 6A-B, lower panel).
106 Absolute biases $|\mu|$ were larger in internal mode (1.84 ± 0.03) as compared to external
107 mode (0.86 ± 0.02 ; $\beta_0 = -0.62 \pm 0.07$, $T(45.62) = -8.38$, $p = 8.59 \times 10^{-11}$; controlling for
108 differences in lapses and thresholds).

109 Lower and upper lapses amounted to $\gamma = 0.13 \pm 2.83 \times 10^{-3}$ and $\delta = 0.1 \pm 2.45 \times 10^{-3}$
110 (Supplemental Figure 6A, C and D). Lapses were larger in internal mode ($\gamma = 0.17 \pm$
111 3.52×10^{-3} , $\delta = 0.14 \pm 3.18 \times 10^{-3}$) as compared to external mode ($\gamma = 0.1 \pm 2.2 \times 10^{-3}$, $\delta =$
112 $0.08 \pm 2 \times 10^{-3}$; $\beta_0 = -0.05 \pm 5.73 \times 10^{-3}$, $T(47.03) = -9.11$, $p = 5.94 \times 10^{-12}$; controlling
113 for differences in biases and thresholds).

114 Conditioning on the previous perceptual choice revealed that the between-mode difference in
115 lapse was not general, but depended on perceptual history: For $y_{t-1} = 0$, only higher lapses δ
116 differed between internal and external mode ($\beta_0 = -0.1 \pm 9.58 \times 10^{-3}$, $T(36.87) = -10.16$, p
117 $= 3.06 \times 10^{-12}$), whereas lower lapses γ did not ($\beta_0 = 0.01 \pm 7.77 \times 10^{-3}$, $T(33.1) = 1.61$, p
118 $= 0.12$). Vice versa, for $y_{t-1} = 1$, lower lapses γ differed between internal and external mode
119 ($\beta_0 = -0.11 \pm 0.01$, $T(40.11) = -9.59$, $p = 6.14 \times 10^{-12}$), whereas higher lapses δ did not
120 ($\beta_0 = 0.01 \pm 7.74 \times 10^{-3}$, $T(33.66) = 1.58$, $p = 0.12$).

121 Thresholds t were estimated at 3 ± 0.06 (Supplemental Figure 6A and E). Thresholds t were
122 larger in internal mode (3.66 ± 0.09) as compared to external mode (2.02 ± 0.03 ; $\beta_0 = -1.77$
123 ± 0.25 , $T(50.45) = -7.14$, $p = 3.48 \times 10^{-9}$; controlling for differences in biases and lapses).

¹²⁴ In contrast to the bias μ and the lapse rates γ and δ , thresholds t were not modulated by
¹²⁵ perceptual history ($\beta_0 = 0.04 \pm 0.06$, $T(2.97 \times 10^3) = 0.73$, $p = 0.47$).

¹²⁶ **1.3.2 Mice**

¹²⁷ When estimated based on the full dataset provided in the IBL database²¹ (i.e., irrespective
¹²⁸ of the preceding perceptual choice y_{t-1}), biases μ were distributed around zero (3.87×10^{-3}
¹²⁹ $\pm 9.81 \times 10^{-3}$; $T(164) = 0.39$, $p = 0.69$; Supplemental Figure 7A-B, upper panel). When
¹³⁰ conditioned on the preceding perceptual choice, biases were negative for $y_{t-1} = 0$ (-0.02
¹³¹ $\pm 8.7 \times 10^{-3}$; $T(164) = -1.99$, $p = 0.05$; Supplemental Figure 7A-B, middle panel) and
¹³² positive for $y_{t-1} = 1$ ($0.02 \pm 9.63 \times 10^{-3}$; $T(164) = 1.91$, $p = 0.06$; Supplemental Figure
¹³³ 7A-B, lower panel). As in humans, mice showed larger biases during internal mode (0.14
¹³⁴ $\pm 7.96 \times 10^{-3}$) as compared to external mode ($0.07 \pm 8.7 \times 10^{-3}$; $\beta_0 = -0.18 \pm 0.03$, $T =$
¹³⁵ -6.38 , $p = 1.77 \times 10^{-9}$; controlling for differences in lapses and thresholds).

¹³⁶ Lower and upper lapses amounted to $\gamma = 0.1 \pm 4.35 \times 10^{-3}$ and $\delta = 0.11 \pm 4.65 \times 10^{-3}$
¹³⁷ (Supplemental Figure 7A, C and D). Lapse rates were higher in internal mode ($\gamma = 0.15 \pm$
¹³⁸ 5.14×10^{-3} , $\delta = 0.16 \pm 5.79 \times 10^{-3}$) as compared to external mode ($\gamma = 0.06 \pm 3.11 \times 10^{-3}$,
¹³⁹ $\delta = 0.07 \pm 3.34 \times 10^{-3}$; $\beta_0 = -0.11 \pm 4.39 \times 10^{-3}$, $T = -24.8$, $p = 4.91 \times 10^{-57}$; controlling
¹⁴⁰ for differences in biases and thresholds).

¹⁴¹ For $y_{t-1} = 0$, the difference between internal and external mode was more pronounced for
¹⁴² higher lapses δ ($T(164) = 21.44$, $p = 1.93 \times 10^{-49}$). Conversely, for $y_{t-1} = 1$, the difference
¹⁴³ between internal and external mode was more pronounced for lower lapses γ ($T(164) =$
¹⁴⁴ -18.24 , $p = 2.68 \times 10^{-41}$). In contrast to the human data, higher lapses δ and lower lapses
¹⁴⁵ γ were significantly elevated during internal mode irrespective of the preceding perceptual
¹⁴⁶ choice (higher lapses δ for $y_{t-1} = 1$: $T(164) = -2.65$, $p = 8.91 \times 10^{-3}$; higher lapses δ for
¹⁴⁷ $y_{t-1} = 0$: $T(164) = -28.29$, $p = 5.62 \times 10^{-65}$; lower lapses γ for $y_{t-1} = 1$: $T(164) = -32.44$, p
¹⁴⁸ $= 2.92 \times 10^{-73}$; lower lapses γ for $y_{t-1} = 0$: $T(164) = -2.5$, $p = 0.01$).

¹⁴⁹ In mice, thresholds t amounted to $0.15 \pm 6.52 \times 10^{-3}$ (Supplemental Figure 7A and E) and
¹⁵⁰ were higher in internal mode (0.27 ± 0.01) as compared to external mode ($0.09 \pm 4.44 \times 10^{-3}$;
¹⁵¹ $\beta_0 = -0.28 \pm 0.04$, $T = -7.26$, $p = 1.53 \times 10^{-11}$; controlling for differences in biases and
¹⁵² lapses). Thresholds t were not modulated by perceptual history ($T(164) = 0.94$, $p = 0.35$).
¹⁵³ In sum, the above analyses showed that, in both humans and mice, internal and external
¹⁵⁴ mode differ with respect to biases, lapses and thresholds. Internally-biased processing was
¹⁵⁵ characterized by higher thresholds, indicating a reduced sensitivity to sensory information,
¹⁵⁶ as well as by larger biases and lapses. Importantly, between-mode differences in biases and
¹⁵⁷ lapses strongly depended on perceptual history. This confirmed that internal mode processing
¹⁵⁸ cannot be explained solely on the ground of a general (i.e., history-independent) increase in
¹⁵⁹ lapses or bias indicative of random or stereotypical responses.

¹⁶⁰ **1.4 Internal mode processing can not be reduced to insufficient 161 task familiarity**

¹⁶² It may be assumed that participants tend to repeat preceding choices when they are not yet
¹⁶³ familiar with the experimental task, leading to history-congruent choices that are caused by
¹⁶⁴ insufficient training. To assess this alternative explanation, we contrasted the correlates of
¹⁶⁵ bimodal inference with training effects in humans and mice.

¹⁶⁶ **1.4.1 Humans**

¹⁶⁷ In the Confidence database²⁰, training effects were visible from RTs that were shortened by
¹⁶⁸ increasing exposure to the task ($\beta = -7.53 \times 10^{-5} \pm 6.32 \times 10^{-7}$, $T(1.81 \times 10^6) = -119.15$, p
¹⁶⁹ $< 2.2 \times 10^{-308}$). Intriguingly, however, history-congruent choices became more frequent with
¹⁷⁰ increased exposure to the task ($\beta = 3.6 \times 10^{-5} \pm 2.54 \times 10^{-6}$, $z = 14.19$, $p = 10^{-45}$), speaking
¹⁷¹ against the proposition that insufficient training induces seriality in response behavior.

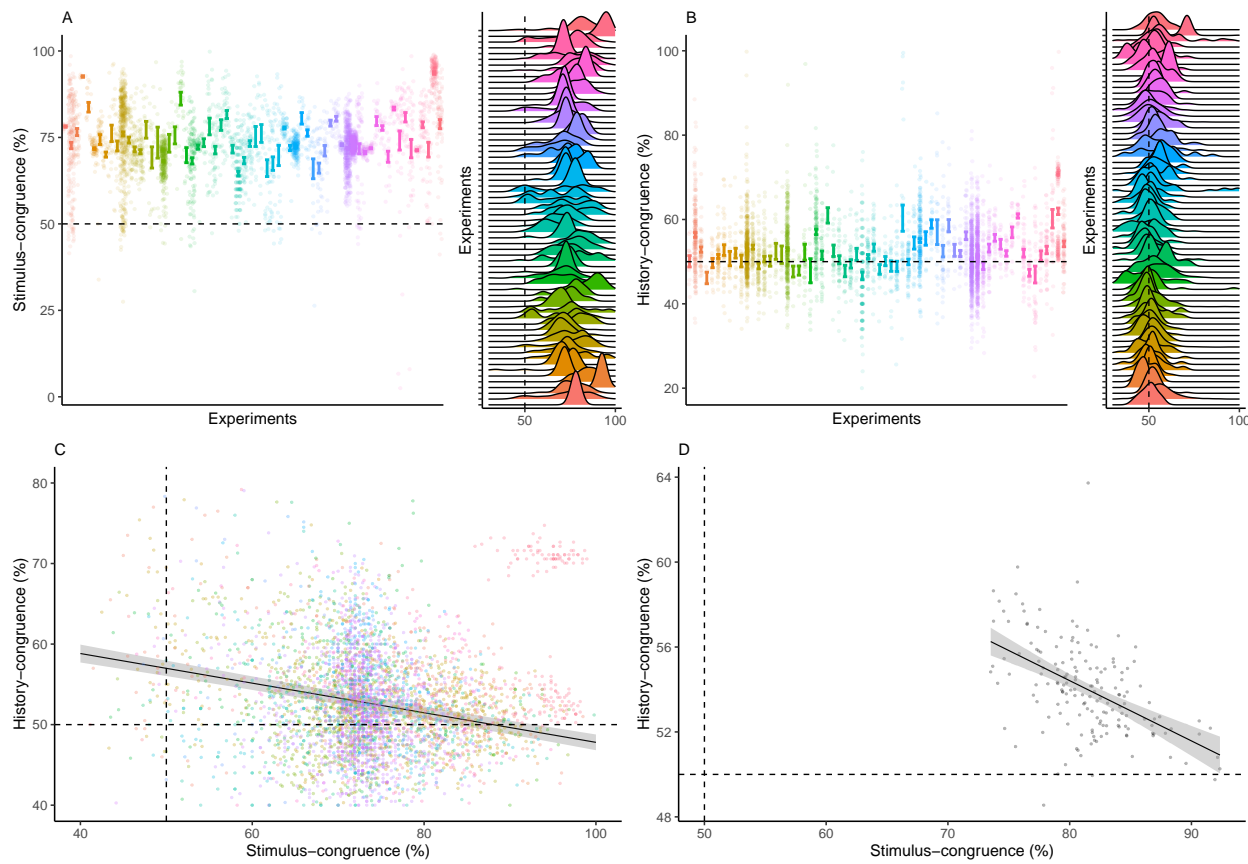
¹⁷² **1.4.2 Mice**

¹⁷³ As in humans, it is an important caveat to consider whether the observed serial dependencies
¹⁷⁴ in mice reflect a phenomenon of perceptual inference, or, alternatively, an unspecific strategy
¹⁷⁵ that occurs at the level of reporting behavior. We reasoned that, if mice indeed tended to
¹⁷⁶ repeat previous choices as a general response pattern, history effects should decrease during
¹⁷⁷ training of the perceptual task. We therefore analyzed how stimulus- and history-congruent
¹⁷⁸ perceptual choices evolved across sessions in mice that, by the end of training, achieved
¹⁷⁹ proficiency (i.e., stimulus-congruence $\geq 80\%$) in the *basic* task of the IBL dataset²¹.

¹⁸⁰ Across sessions, we found that stimulus-congruent perceptual choices became more frequent
¹⁸¹ ($\beta = 0.34 \pm 7.13 \times 10^{-3}$, $T(8.51 \times 10^3) = 47.66$, $p < 2.2 \times 10^{-308}$) and TDs were progressively
¹⁸² shortened ($\beta = -22.14 \pm 17.06$, $T(1.14 \times 10^3) = -1.3$, $p < 2.2 \times 10^{-308}$). Crucially, the
¹⁸³ frequency of history-congruent perceptual choices also increased during training ($\beta = 0.13 \pm$
¹⁸⁴ 4.67×10^{-3} , $T(8.4 \times 10^3) = 27.04$, $p = 1.96 \times 10^{-154}$; Supplemental Figure S8).

¹⁸⁵ Within individual session, longer task exposure was associated with an increase in history-
¹⁸⁶ congruence ($\beta = 3.6 \times 10^{-5} \pm 2.54 \times 10^{-6}$, $z = 14.19$, $p = 10^{-45}$) and a decrease in TDs (β
¹⁸⁷ $= -0.1 \pm 3.96 \times 10^{-3}$, $T(1.34 \times 10^6) = -24.99$, $p = 9.45 \times 10^{-138}$). In sum, these findings
¹⁸⁸ strongly argue against the proposition that mice show biases toward perceptual history due
¹⁸⁹ to an unspecific response strategy.

190 **1.5 Supplemental Figure S1**



191

192 **Supplemental Figure S1. Stimulus- and history-congruence.**

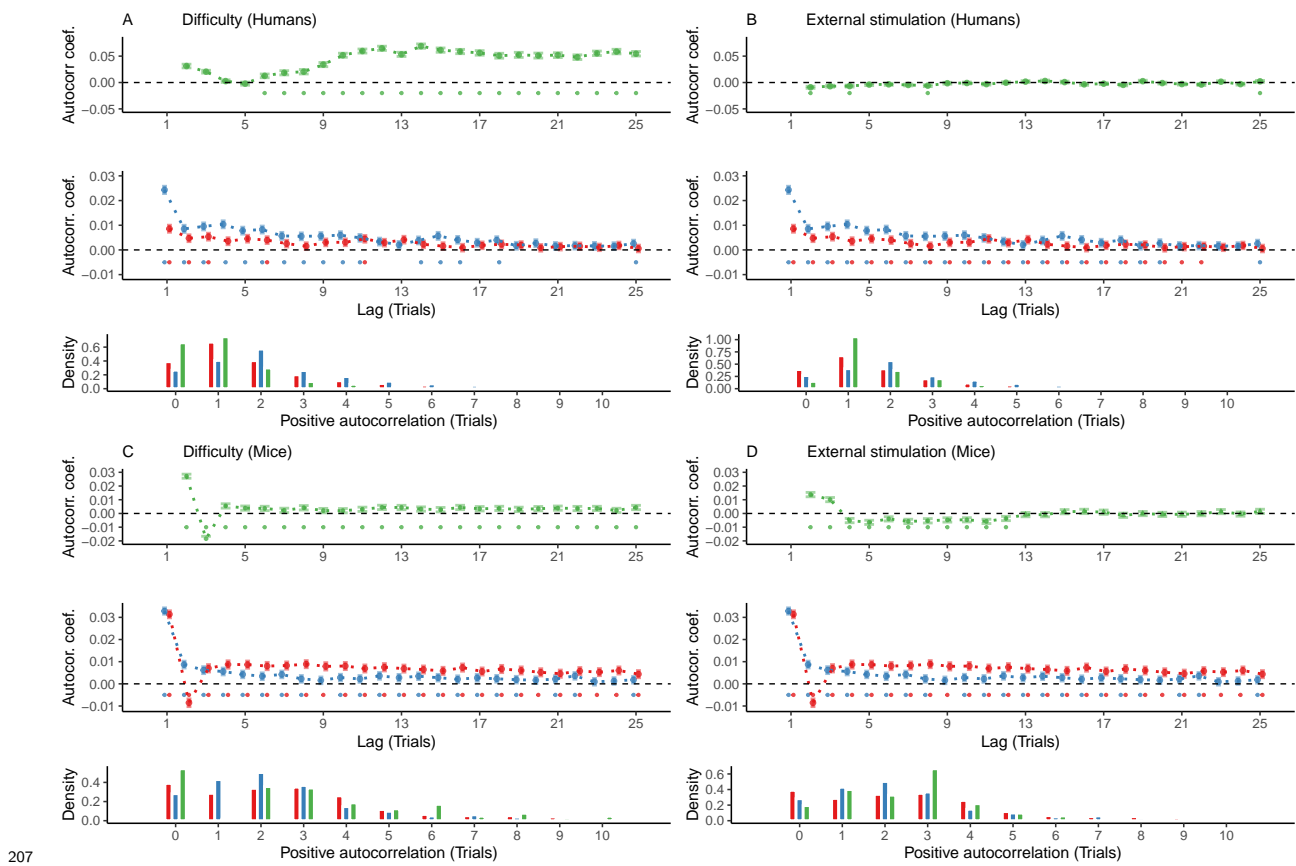
193 A. Stimulus-congruent choices in humans amounted to $73.46\% \pm 0.15\%$ of trials and were
194 highly consistent across the experiments selected from the Confidence Database.

195 B. History-congruent choices in humans amounted to $52.7\% \pm 0.12\%$ of trials. In analogy
196 to stimulus-congruence, the prevalence of history-congruence was highly consistent across
197 the experiments selected from the Confidence Database. 48.48% of experiments showed
198 significant ($p < 0.05$) biases toward preceding choices, whereas 2 of the 66 of the included
199 experiments showed significant repelling biases.

200 C. In humans, we found an enhanced impact of perceptual history in participants who were
201 less sensitive to external sensory information ($T(4.3 \times 10^3) = -14.27$, $p = 3.78 \times 10^{-45}$),
202 suggesting that perception results from the competition of external with internal information.

²⁰³ D. In analogy to humans, mice that were less sensitive to external sensory information
²⁰⁴ showed stronger biases toward perceptual history ($T(163) = -7.52$, $p = 3.44 \times 10^{-12}$, Pearson
²⁰⁵ correlation).

206 **1.6 Supplemental Figure S2**



207

208 **Supplemental Figure S2. Controlling for task difficulty and external stimulation.**

209 In this study, we found highly significant autocorrelations of stimulus- and history-congruence
 210 in humans as well as in mice, while controlling for task difficulty and the sequence of external
 211 stimulation. Here, we confirm that the autocorrelations of stimulus- and history-congruence
 212 were not a trivial consequence of the experimental design or the addition of tast difficulty and
 213 external stimulation as control variables in the computation of group-level autocorrelations.

214 A. In humans, task difficulty (in green) showed a significant autocorrelation starting at the
 215 5th trial (upper panel, dots at the bottom indicate intercepts $\neq 0$ in trial-wise linear mixed
 216 effects modeling at $p < 0.05$). When controlling for task difficulty only, linear mixed effects
 217 modeling indicated a significant autocorrelation of stimulus-congruence (in red) for the first 3
 218 consecutive trials (middle panel). 20% of trials within the displayed time window remained
 219 significantly autocorrelated. The autocorrelation of history-congruence (in blue) remained

²²⁰ significant for the first 11 consecutive trials (64% significantly autocorrelated trials within
²²¹ the displayed time window). At the level of individual participants, the autocorrelation of
²²² task difficulty exceeded the respective autocorrelation of randomly permuted within a lag of
²²³ $21.66 \pm 8.37 \times 10^{-3}$ trials (lower panel).

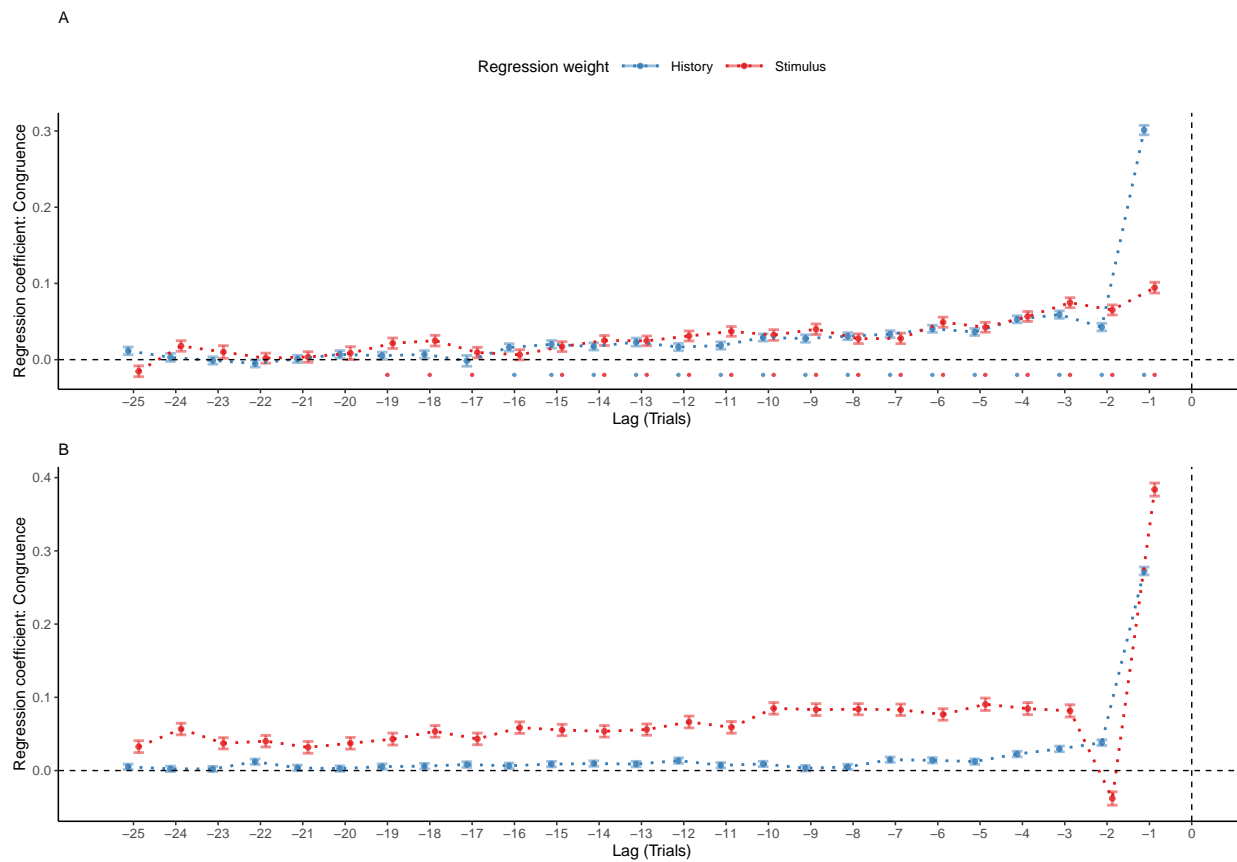
²²⁴ B. In humans, the sequence of external stimulation (i.e., which of the two binary outcomes
²²⁵ was supported by the presented stimuli; depicted in green) was negatively autocorrelated
²²⁶ for 1 trial. When controlling for the autocorrelation of external stimulation only, stimulus-
²²⁷ congruence remained significantly autocorrelated for 22 consecutive trials (88% of trials
²²⁸ within the displayed time window; lower panel) and history-congruence remained significantly
²²⁹ autocorrelated for 20 consecutive trials (84% of trials within the displayed time window). At
²³⁰ the level of individual participants, the autocorrelation of external stimulation exceeded the
²³¹ respective autocorrelation of randomly permuted within a lag of $2.94 \pm 4.4 \times 10^{-3}$ consecutive
²³² trials (lower panel).

²³³ C. In mice, task difficulty showed a significant autocorrelated for the first 25 consecutive trials
²³⁴ (upper panel). When controlling only for task difficulty only, linear mixed effects modeling
²³⁵ indicated a significant autocorrelation of stimulus-congruence for the first 36 consecutive trials
²³⁶ (middle panel). In total, 100% of trials within the displayed time window remained significantly
²³⁷ autocorrelated. The autocorrelation of history-congruence remained significant for the first
²³⁸ 8 consecutive trials, with 84% significantly autocorrelated trials within the displayed time
²³⁹ window. At the level of individual mice, autocorrelation coefficients for difficulty were elevated
²⁴⁰ above randomly permuted data within a lag of 15.13 ± 0.19 consecutive trials (lower panel).

²⁴¹ D. In mice, the sequence of external stimulation (i.e., which of the two binary outcomes was
²⁴² supported by the presented stimuli) was negatively autocorrelated for 11 consecutive trials
²⁴³ (upper panel). When controlling only for the autocorrelation of external stimulation, stimulus-
²⁴⁴ congruence remained significantly autocorrelated for 86 consecutive trials (100% of trials
²⁴⁵ within the displayed time window; middle) and history-congruence remained significantly

²⁴⁶ autocorrelated for 8 consecutive trials (84% of trials within the displayed time window). At
²⁴⁷ the level of individual mice, autocorrelation coefficients for external stimulation were elevated
²⁴⁸ above randomly permuted data within a lag of $2.53 \pm 9.8 \times 10^{-3}$ consecutive trials (lower
²⁴⁹ panel).

250 **1.7 Supplemental Figure S3**



251

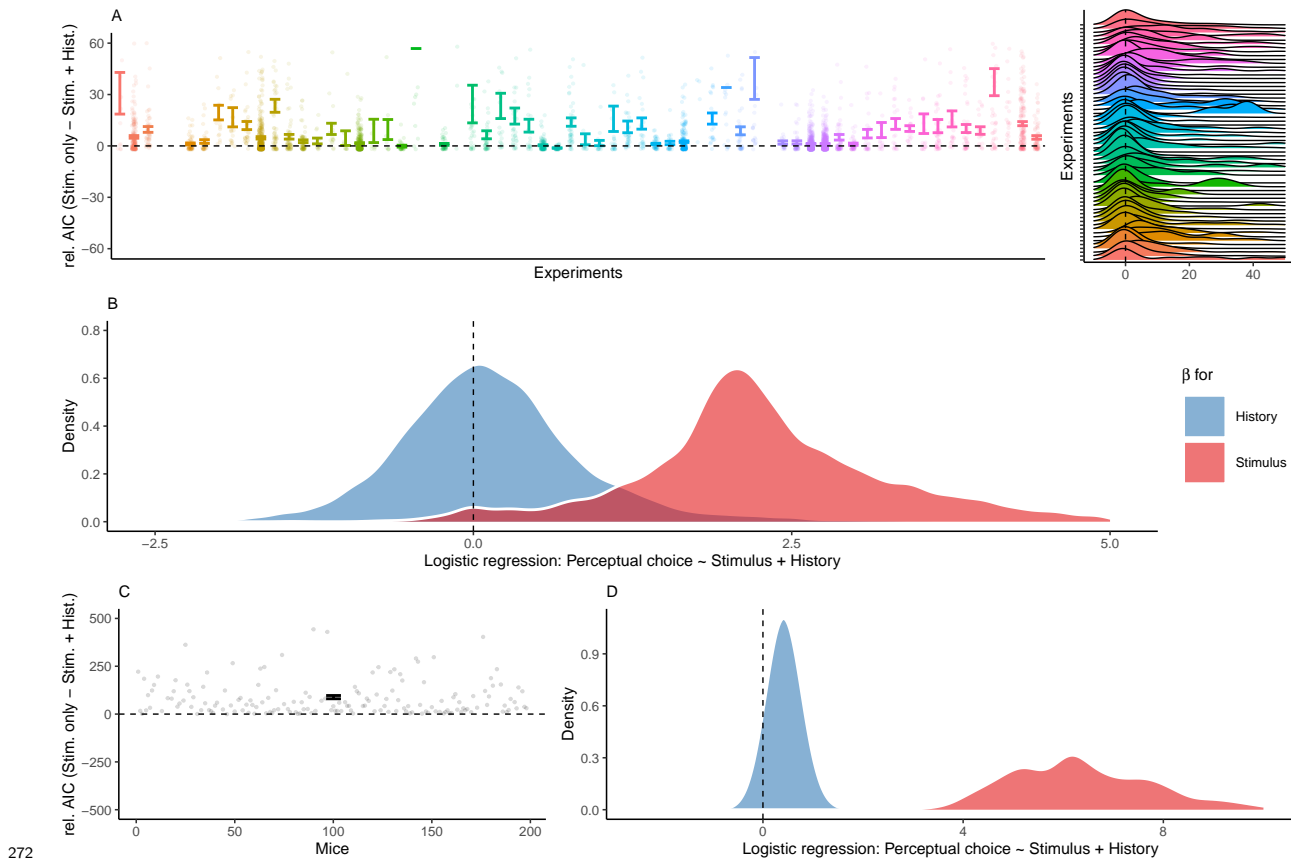
252 **Supplemental Figure S3. Reproducing group-level autocorrelations using logistic**
253 **regression.**

254 A. As an alternative to group-level autocorrelation coefficients, we used trial-wise logistic
255 regression to quantify serial dependencies in stimulus- and history-congruence. This analysis
256 predicted stimulus- and history-congruence at the index trial (trial $t = 0$, vertical line) based
257 on stimulus- and history-congruence at the 100 preceding trials. Mirroring the shape of the
258 group-level autocorrelations, trial-wise regression coefficients (depicted as mean \pm SEM, dots
259 mark trials with regression weights significantly greater than zero at $p < 0.05$) increased
260 toward the index trial $t = 0$ for the human data.

261 B. Following our results in human data, regression coefficients that predicted history-
262 congruence at the index trial (trial $t = 0$, vertical line) increased exponentially for trials
263 closer to the index trial in mice. In contrast to history-congruence, stimulus-congruence

²⁶⁴ showed a negative regression weight (or autocorrelation coefficient; Figure 3B) at trial -2.
²⁶⁵ This was due to the experimental design (see also the autocorrelations of difficulty and
²⁶⁶ external stimulation in Supplemental Figure S2C and D): When mice made errors at easy
²⁶⁷ trials (contrast $\geq 50\%$), the upcoming stimulus was shown at the same spatial location and at
²⁶⁸ high contrast. This increased the probability of stimulus-congruent perceptual choices after
²⁶⁹ stimulus-incongruent perceptual choices at easy trials, thereby creating a negative regression
²⁷⁰ weight (or autocorrelation coefficient) of stimulus-congruence at trial -2.

271 **1.8 Supplemental Figure S4**



272 **273 Supplemental Figure S4. History-congruence in logistic regression.**

274 A. To ensure that perceptual history played a significant role in perception despite the ongoing
 275 stream of external information, we tested whether human perceptual decision-making was
 276 better explained by the combination of external and internal information or, alternatively,
 277 by external information alone. To this end, we compared AIC between logistic regression
 278 models that predicted trial-wise perceptual responses either by both current external sensory
 279 information and the preceding percept, or by external sensory information alone (values above
 280 zero indicate a superiority of the full model). With high consistency across the experiments
 281 selected from the Confidence Database, this model-comparison confirmed that perceptual
 282 history contributed significantly to perception (difference in AIC = 8.07 ± 0.53 , T(57.22) =
 283 4.1, $p = 1.31 \times 10^{-4}$).

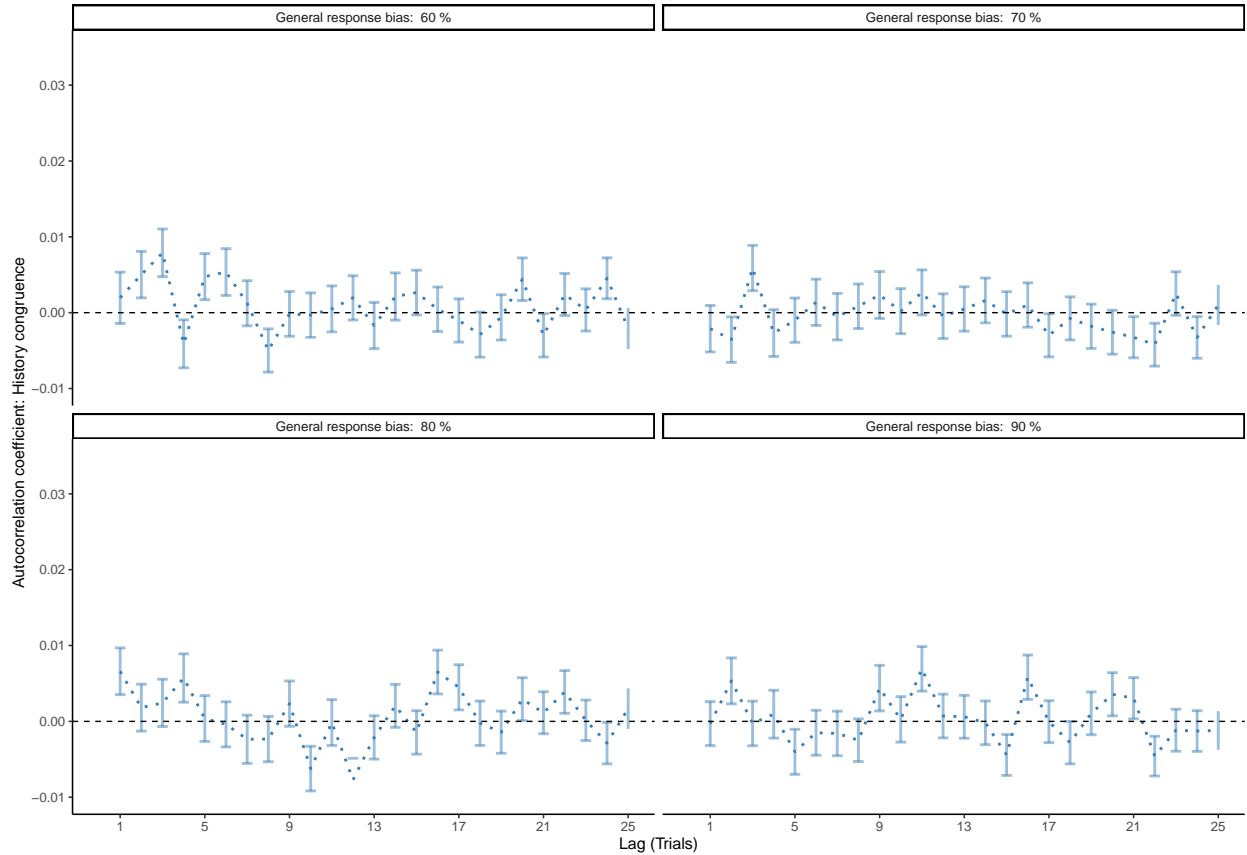
284 B. Participant-wise regression coefficients amount to 0.18 ± 0.02 for the effect of perceptual

²⁸⁵ history and 2.51 ± 0.03 for external sensory stimulation.

²⁸⁶ C. In mice, an AIC-based model comparison indicated that perception was better explained
²⁸⁷ by logistic regression models that predicted trial-wise perceptual responses based on both
²⁸⁸ current external sensory information and the preceding percept (difference in AIC = $88.62 \pm$
²⁸⁹ 8.57 , $T(164) = -10.34$, $p = 1.29 \times 10^{-19}$).

²⁹⁰ D. In mice, individual regression coefficients amounted to 0.42 ± 0.02 for the effect of
²⁹¹ perceptual history and 6.91 ± 0.21 for external sensory stimulation.

292 **1.9 Supplemental Figure S5**



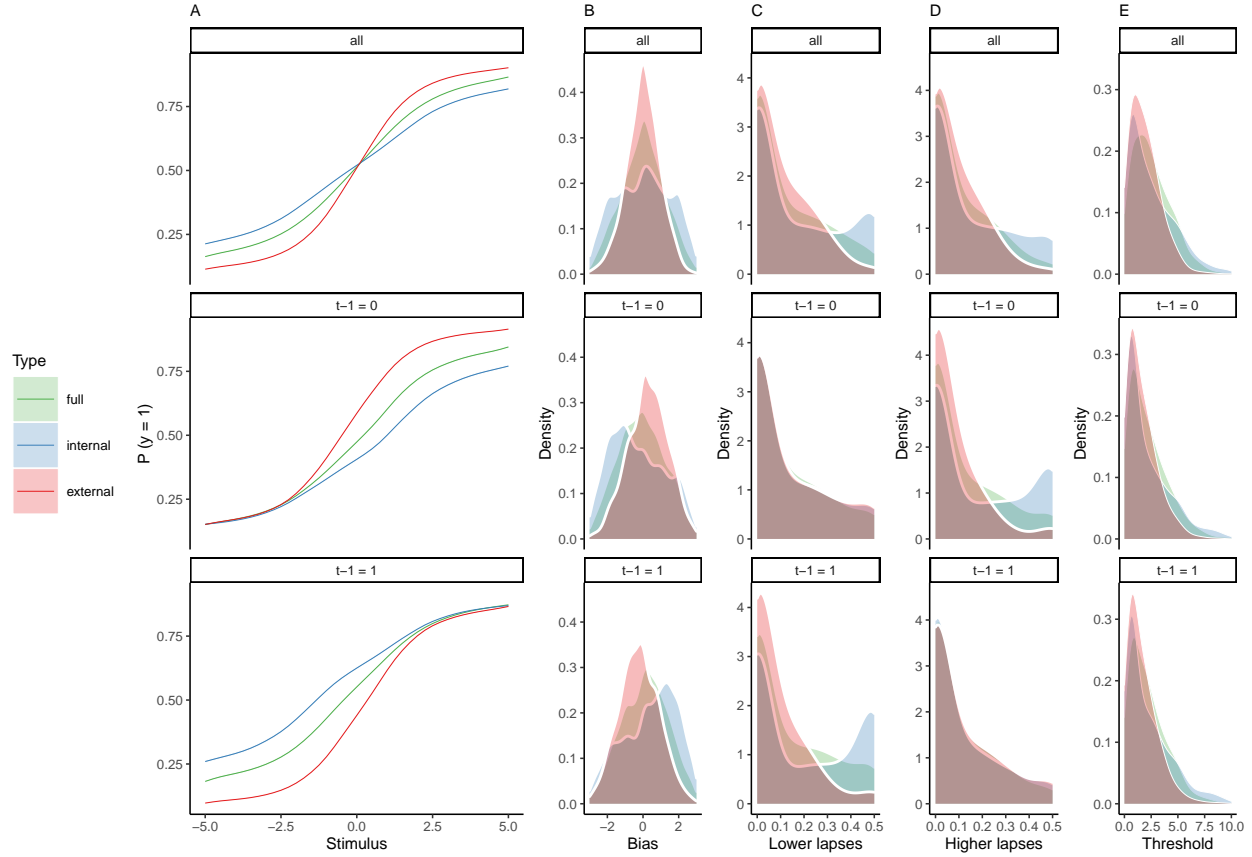
293

294 **Supplemental Figure S5. Correcting for general response biases.**

295 Here, we ask whether the autocorrelation of history-congruence (as shown in Figure 2-3C)
 296 may be driven by general response biases (i.e., a general propensity to choose one of the two
 297 possible outcomes more frequently than the alternative). To this end, we generated sequences
 298 of 100 perceptual choices with general response biases ranging from 60 to 90% for 1000
 299 simulated participants each. We then computed the autocorrelation of history-congruence
 300 for these simulated data. Crucially, we used the correction procedure that is applied to the
 301 autocorrelation curves shown in this manuscript: All reported autocorrelation coefficients are
 302 computed relative to the average autocorrelation coefficients obtained for 100 iterations of
 303 randomly permuted trial sequences. The above simulation show that this correction procedure
 304 removes any potential contribution of general response biases to the autocorrelation of history-
 305 congruence. This indicates that the autocorrelation of history-congruence (as shown in Figure

³⁰⁶ 2-3C) is not driven by general response biases that were present in the empirical data at a
³⁰⁷ level of $58.71\% \pm 0.22\%$ in humans and $54.6\% \pm 0.3\%$ in mice.

308 **1.10 Supplemental Figure S6**



309

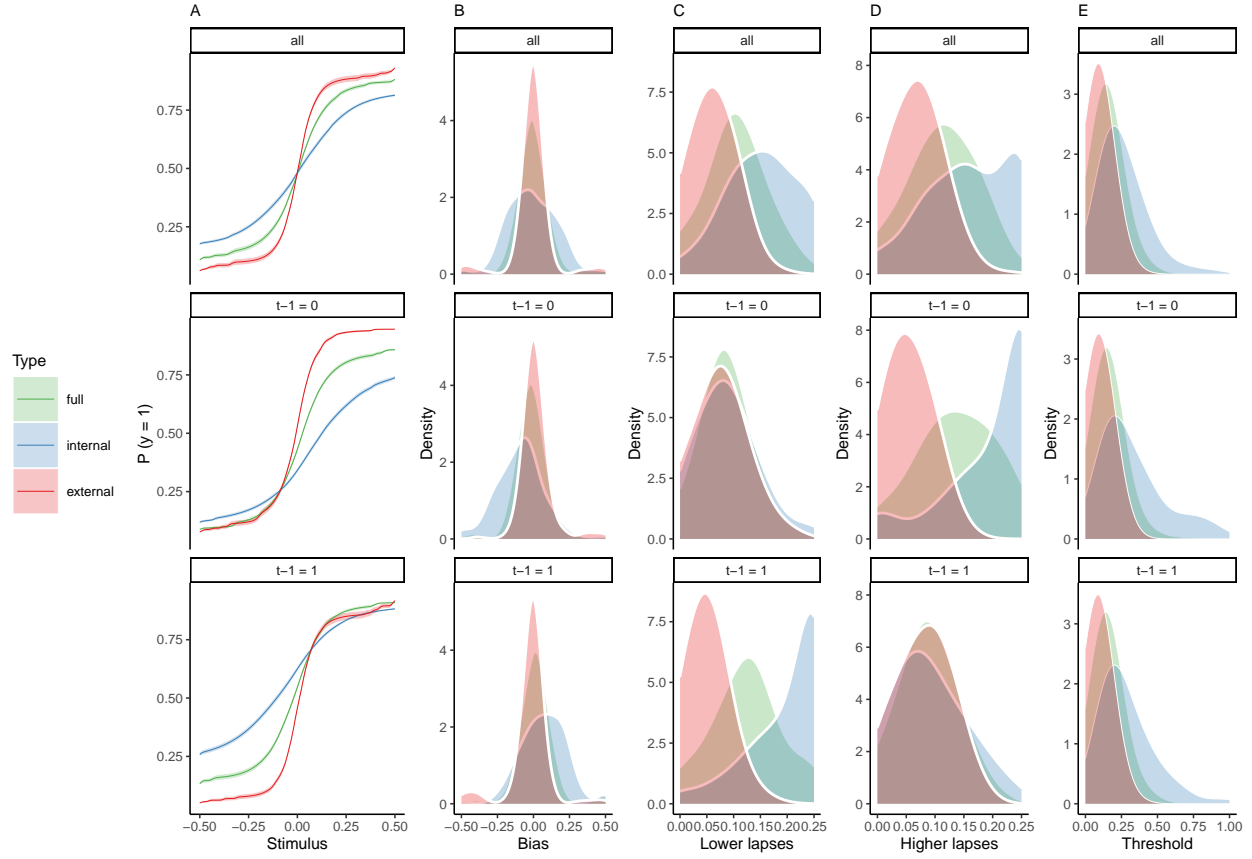
310 **Supplemental Figure S6. Full and history-conditioned psychometric functions**
 311 **across modes in humans.**

312 A. Here, we show average psychometric functions for the full dataset (upper panel) and
 313 conditioned on perceptual history ($y_{t-1} = 1$ and $y_{t-1} = 0$; middle and lower panel) across
 314 modes (green line) and for internal mode (blue line) and external mode (red line) separately.

315 B. Across the full dataset, biases μ were distributed around zero ($\beta_0 = 7.37 \times 10^{-3} \pm 0.09$,
 316 $T(36.8) = 0.08$, $p = 0.94$; upper panel), with larger absolute biases $|\mu|$ for internal as compared
 317 to external mode ($\beta_0 = -0.62 \pm 0.07$, $T(45.62) = -8.38$, $p = 8.59 \times 10^{-11}$; controlling for
 318 differences in lapses and thresholds). When conditioned on perceptual history, we observed
 319 negative biases for $y_{t-1} = 0$ ($\beta_0 = 0.56 \pm 0.12$, $T(43.39) = 4.6$, $p = 3.64 \times 10^{-5}$; middle
 320 panel) and positive biases for $y_{t-1} = 1$ ($\beta_0 = 0.56 \pm 0.12$, $T(43.39) = 4.6$, $p = 3.64 \times 10^{-5}$;
 321 lower panel).

- 322 C. Lapse rates were higher in internal mode as compared to external mode ($\beta_0 = -0.05 \pm$
323 5.73×10^{-3} , $T(47.03) = -9.11$, $p = 5.94 \times 10^{-12}$; controlling for differences in biases and
324 thresholds; see upper panel and subplot D). Importantly, the between-mode difference in
325 lapses depended on perceptual history: We found no significant difference in lower lapses
326 γ for $y_{t-1} = 0$ ($\beta_0 = 0.01 \pm 7.77 \times 10^{-3}$, $T(33.1) = 1.61$, $p = 0.12$; middle panel), but a
327 significant difference for $y_{t-1} = 1$ ($\beta_0 = -0.11 \pm 0.01$, $T(40.11) = -9.59$, $p = 6.14 \times 10^{-12}$;
328 lower panel).
- 329 D. Conversely, higher lapses δ were significantly increased for $y_{t-1} = 0$ ($\beta_0 = -0.1 \pm$
330 9.58×10^{-3} , $T(36.87) = -10.16$, $p = 3.06 \times 10^{-12}$; middle panel), but not for $y_{t-1} = 1$ ($\beta_0 =$
331 $0.01 \pm 7.74 \times 10^{-3}$, $T(33.66) = 1.58$, $p = 0.12$; lower panel).
- 332 E. The thresholds t were larger in internal as compared to external mode ($\beta_0 = -1.77 \pm 0.25$,
333 $T(50.45) = -7.14$, $p = 3.48 \times 10^{-9}$; controlling for differences in biases and lapses) and were
334 not modulated by perceptual history ($\beta_0 = 0.04 \pm 0.06$, $T(2.97 \times 10^3) = 0.73$, $p = 0.47$).

335 **1.11 Supplemental Figure S7**



336

337 **Supplemental Figure S7. Full and history-conditioned psychometric functions**
 338 **across modes in mice.**

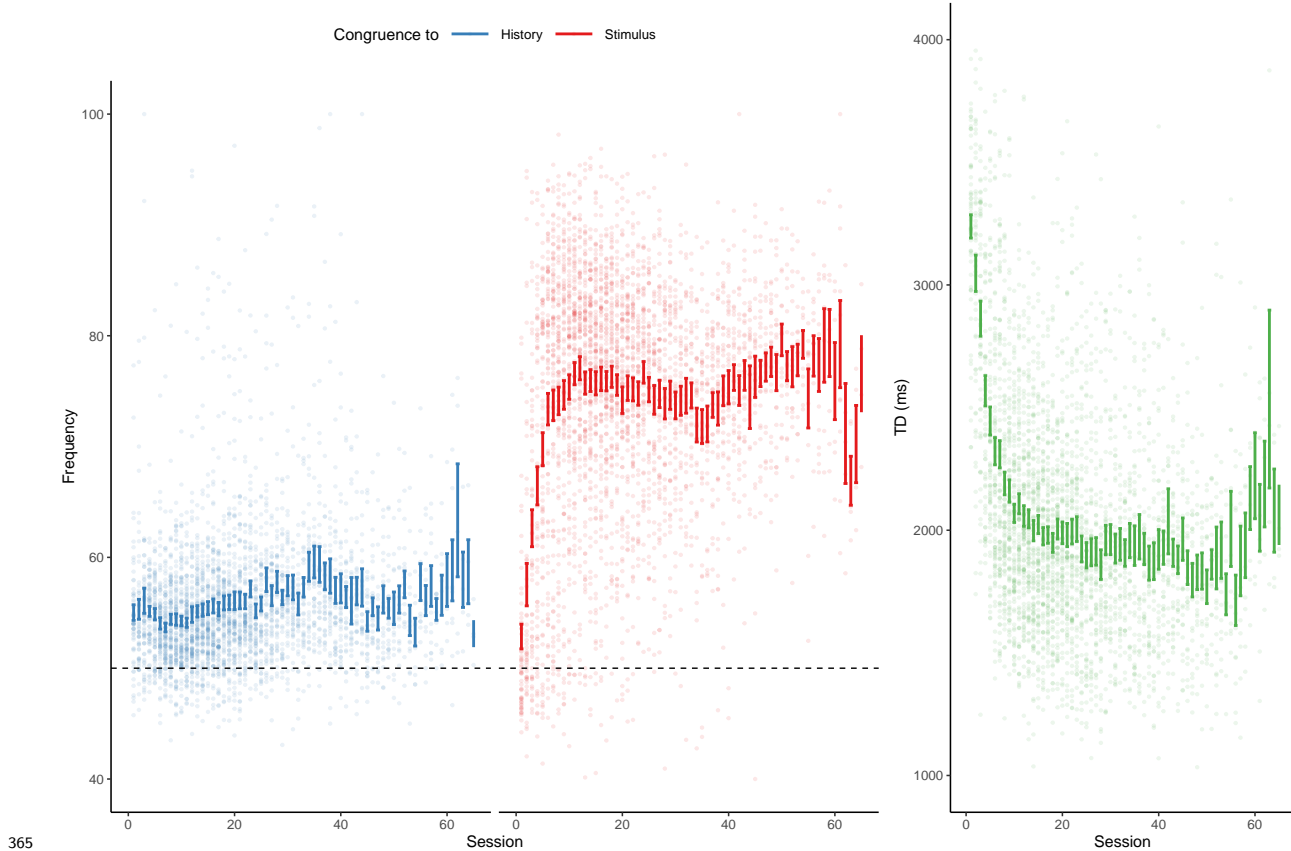
- 339 A. Here, we show average psychometric functions for the full IBL dataset (upper panel) and
 340 conditioned on perceptual history ($y_{t-1} = 1$ and $y_{t-1} = 0$; middle and lower panel) across
 341 modes (green line) and for internal mode (blue line) and external mode (red line) separately.
 342 B. Across the full dataset, biases μ were distributed around zero ($T(164) = 0.39$, $p = 0.69$;
 343 upper panel), with larger absolute biases $|\mu|$ for internal as compared to external mode ($\beta_0 =$
 344 -0.18 ± 0.03 , $T = -6.38$, $p = 1.77 \times 10^{-9}$; controlling for differences in lapses and thresholds).
 345 When conditioned on perceptual history, we observed negative biases for $y_{t-1} = 0$ ($T(164)$
 346 $= -1.99$, $p = 0.05$; middle panel) and positive biases for $y_{t-1} = 1$ ($T(164) = 1.91$, $p = 0.06$;
 347 lower panel).

³⁴⁸ C. Lapse rates were higher in internal as compared to external mode ($\beta_0 = -0.11 \pm 4.39 \times 10^{-3}$,
³⁴⁹ $T = -24.8$, $p = 4.91 \times 10^{-57}$; controlling for differences in biases and thresholds; upper
³⁵⁰ panel, see subplot D). For $y_{t-1} = 1$, the difference between internal and external mode was
³⁵¹ more pronounced for lower lapses γ ($T(164) = -18.24$, $p = 2.68 \times 10^{-41}$) as compared to
³⁵² higher lapses δ (see subplot D). In mice, lower lapses γ were significantly elevated during
³⁵³ internal mode irrespective of the preceding perceptual choice (middle panel: lower lapses γ
³⁵⁴ for $y_{t-1} = 0$; $T(164) = -2.5$, $p = 0.01$, lower panel: lower lapses γ for $y_{t-1} = 1$; $T(164) =$
³⁵⁵ -32.44 , $p = 2.92 \times 10^{-73}$).

³⁵⁶ D. For $y_{t-1} = 0$, the difference between internal and external mode was more pronounced
³⁵⁷ for higher lapses δ ($T(164) = 21.44$, $p = 1.93 \times 10^{-49}$, see subplot C). Higher lapses were
³⁵⁸ significantly elevated during internal mode irrespective of the preceding perceptual choice
³⁵⁹ (middle panel: higher lapses δ for $y_{t-1} = 0$; $T(164) = -28.29$, $p = 5.62 \times 10^{-65}$ lower panel:
³⁶⁰ higher lapses δ for $y_{t-1} = 1$; $T(164) = -2.65$, $p = 8.91 \times 10^{-3}$;).

³⁶¹ E. Thresholds t were higher in internal as compared to external mode ($\beta_0 = -0.28 \pm 0.04$,
³⁶² $T = -7.26$, $p = 1.53 \times 10^{-11}$; controlling for differences in biases and lapses) and were not
³⁶³ modulated by perceptual history ($T(164) = 0.94$, $p = 0.35$).

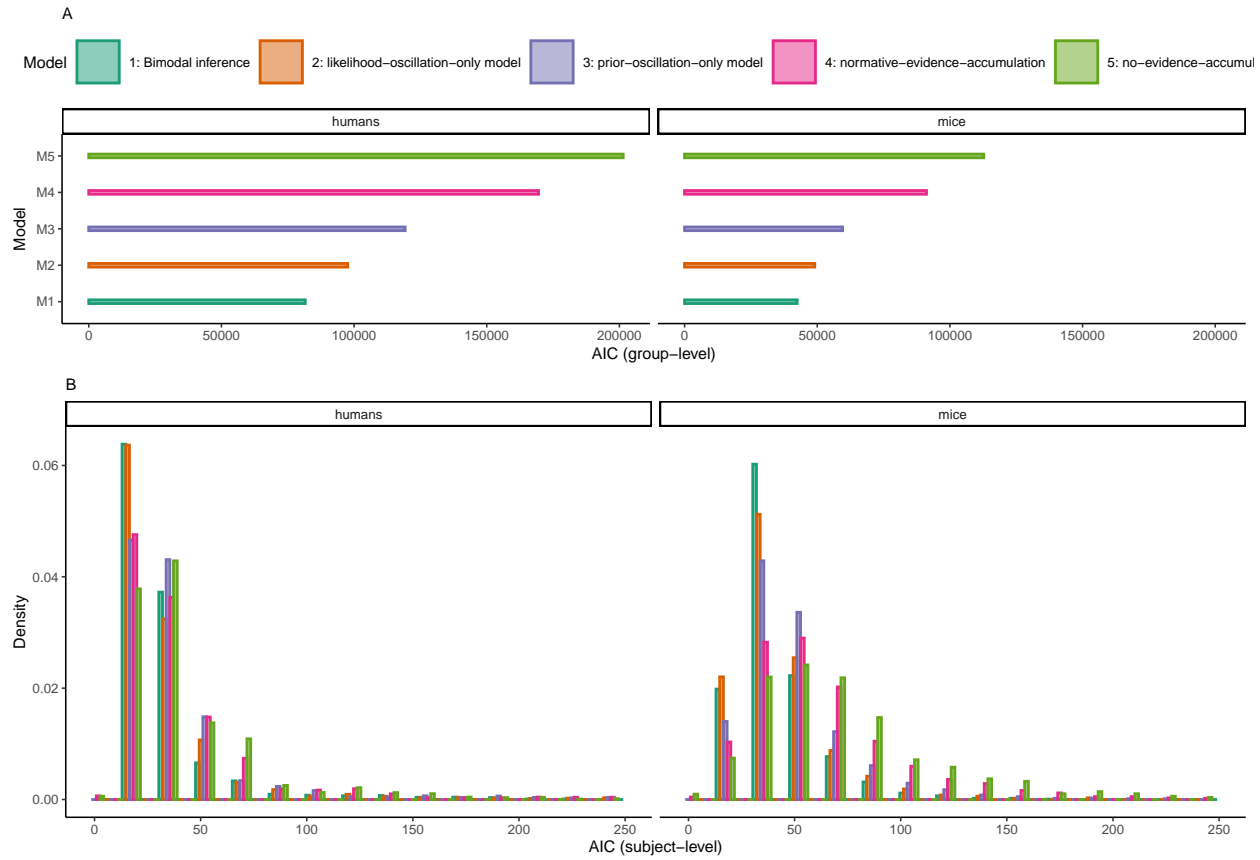
³⁶⁴ **1.12 Supplemental Figure S8**



³⁶⁵ **366 Supplemental Figure S8. History-/stimulus-congruence and TDs during training
367 of the basic task.**

³⁶⁸ Here, we depict the progression of history- and stimulus-congruence (depicted in blue and
³⁶⁹ red, respectively; left panel) as well as TDs (in green; right panel) across training sessions in
³⁷⁰ mice that achieved proficiency (i.e., stimulus-congruence $\geq 80\%$) in the *basic* task of the IBL
³⁷¹ dataset. We found that both history-congruent perceptual choices ($\beta = 0.13 \pm 4.67 \times 10^{-3}$,
³⁷² $T(8.4 \times 10^3) = 27.04$, $p = 1.96 \times 10^{-154}$) and stimulus-congruent perceptual choices ($\beta =$
³⁷³ $0.34 \pm 7.13 \times 10^{-3}$, $T(8.51 \times 10^3) = 47.66$, $p < 2.2 \times 10^{-308}$) became more frequent with
³⁷⁴ training. As in humans, mice showed shorter TDs with increased exposure to the task ($\beta =$
³⁷⁵ -22.14 ± 17.06 , $T(1.14 \times 10^3) = -1.3$, $p < 2.2 \times 10^{-308}$).

376 **1.13 Supplemental Figure S9**



377

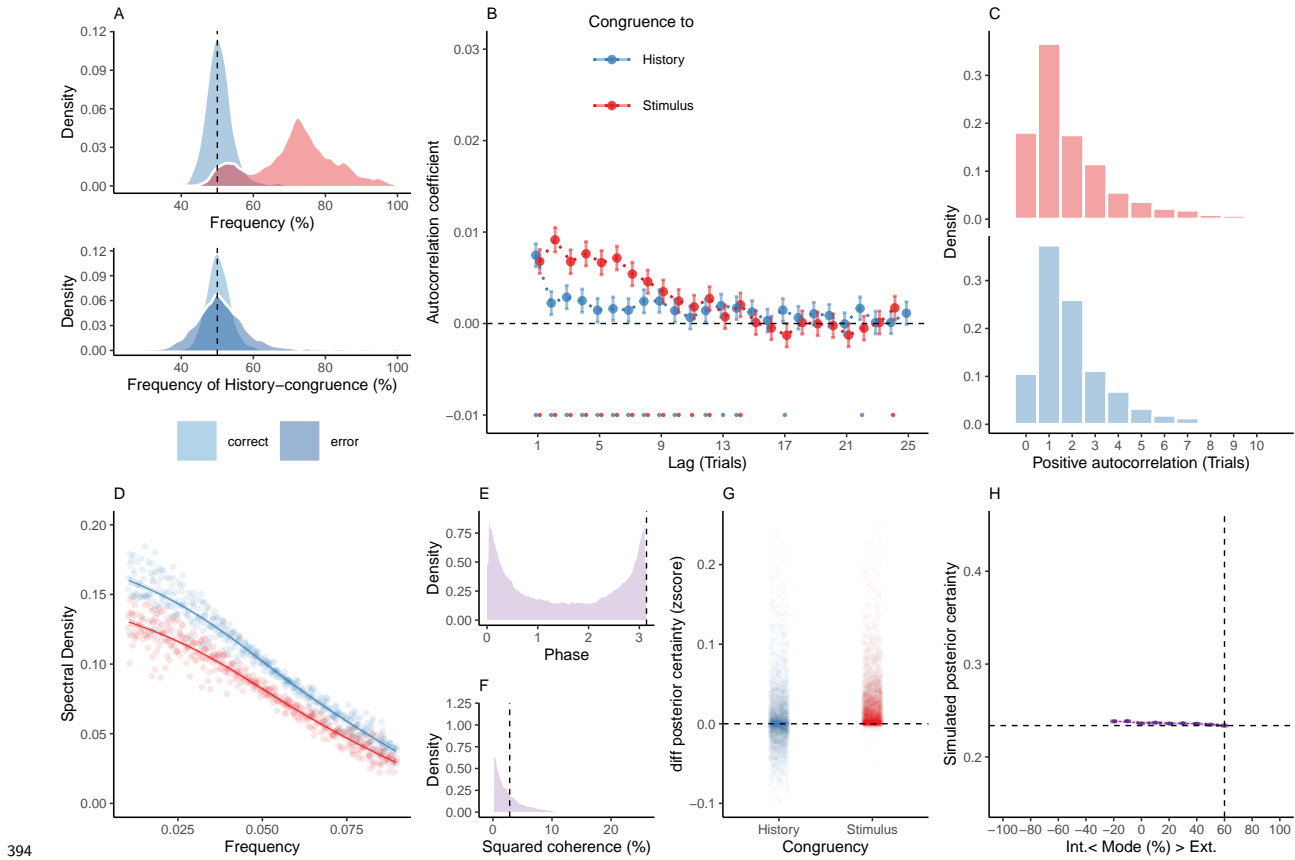
378 **Supplemental Figure S9. Comparison of the bimodal inference model against**
379 **reduced control models.**

380 A. Group-level AIC. The bimodal inference model (M1) achieved the lowest AIC across the
381 full model space ($AIC_1 = 8.16 \times 10^4$ in humans and 4.24×10^4 in mice). Model M2 ($AIC_2 =$
382 9.76×10^4 in humans and 4.91×10^4 in mice) and Model M3 ($AIC_3 = 1.19 \times 10^5$ in humans
383 and 5.95×10^4 in mice) incorporated only oscillations of either likelihood or prior precision.
384 Model M4 ($AIC_4 = 1.69 \times 10^5$ in humans and 9.12×10^4 in mice) lacked any oscillations of
385 likelihood and prior precision and corresponded to the normative model proposed by Glaze et
386 al.⁵¹. In model M5 ($AIC_5 = 2.01 \times 10^5$ in humans and 1.13×10^5 in mice), we furthermore
387 removed the integration of information across trials, such that perception depended only in
388 incoming sensory information.

389 B. Subject-level AIC. Here, we show the distribution of AIC values at the subject-level.

³⁹⁰ AIC for the bimodal inference model tended to be smaller than AIC for the comparator
³⁹¹ models (statistical comparison to the second-best model M2 in humans: $\beta = -1.71 \pm 0.19$,
³⁹² $T(8.57 \times 10^3) = -8.85$, $p = 1.06 \times 10^{-18}$; mice: $T(1.57 \times 10^3) = -3.08$, $p = 2.12 \times 10^{-3}$).

393 **1.14 Supplemental Figure S10**



394 **Supplemental Figure S10. Reduced Control Model M2: Only oscillation of the likelihood.** When simulating data for the *likelihood-oscillation-only model*, we removed the oscillation from the prior term by setting the amplitude a_ψ to zero. Simulated data thus depended only on the participant-wise estimates for hazard rate H , amplitude a_{LLR} , frequency f , phase p and inverse decision temperature ζ .

400 A. Similar to the full model M1 (Figure 1F and Figure 4), simulated perceptual choices
 401 were stimulus-congruent in $71.97\% \pm 0.17\%$ of trials (in red). History-congruent amounted
 402 to $50.76\% \pm 0.07\%$ of trials (in blue). As in the full model, the likelihood-oscillation-only
 403 model showed a significant bias toward perceptual history $T(4.32 \times 10^3) = 10.29$, $p =$
 404 1.54×10^{-24} ; upper panel). Similarly, history-congruent choices were more frequent at error
 405 trials ($T(4.32 \times 10^3) = 9.71$, $p = 4.6 \times 10^{-22}$; lower panel).

406 B. In the likelihood-oscillation-only model, we observed that the autocorrelation coefficients for

407 history-congruence were reduced below the autocorrelation coefficients of stimulus-congruence.
408 This is an approximately five-fold reduction relative to the empirical results observed in humans
409 (Figure 2B), where the autocorrelation of history-congruence was above the autocorrelation of
410 stimulus-congruence. Moreover, in the reduced model shown here, the number of consecutive
411 trials that showed significant autocorrelation of history-congruence was reduced to 11.

412 C. In the likelihood-oscillation-only model, the number of consecutive trials at which true
413 autocorrelation coefficients exceeded the autocorrelation coefficients for randomly permuted
414 data did not differ with respect to stimulus-congruence ($2.62 \pm 1.39 \times 10^{-3}$ trials; $T(4.32 \times 10^3)$
415 = 1.85, $p = 0.06$), but decreased with respect to history-congruence ($2.4 \pm 8.45 \times 10^{-4}$ trials;
416 $T(4.32 \times 10^3) = -15.26$, $p = 3.11 \times 10^{-51}$) relative to the full model.

417 D. In the likelihood-oscillation-only model, the smoothed probabilities of stimulus- and
418 history-congruence (sliding windows of ± 5 trials) fluctuated as a scale-invariant process with
419 a $1/f$ power law, i.e., at power densities that were inversely proportional to the frequency
420 (power $\sim 1/f^\beta$; stimulus-congruence: $\beta = -0.81 \pm 1.17 \times 10^{-3}$, $T(1.92 \times 10^5) = -688.65$, $p <$
421 2.2×10^{-308} ; history-congruence: $\beta = -0.79 \pm 1.14 \times 10^{-3}$, $T(1.92 \times 10^5) = -698.13$, $p <$
422 2.2×10^{-308}).

423 E. In the likelihood-oscillation-only model, the distribution of phase shift between fluctuations
424 in simulated stimulus- and history-congruence peaked at half a cycle (π denoted by dotted
425 line). In contrast to the full model, the dynamic probabilities of simulated stimulus- and
426 history-congruence were positively correlated ($\beta = 2.7 \times 10^{-3} \pm 7.6 \times 10^{-4}$, $T(2.02 \times 10^6) =$
427 3.55 , $p = 3.8 \times 10^{-4}$).

428 F. In the likelihood-oscillation-only model, the average squared coherence between fluctuations
429 in simulated stimulus- and history-congruence (black dotted line) was reduced in comparison
430 to the full model ($T(3.51 \times 10^3) = -4.56$, $p = 5.27 \times 10^{-6}$) and amounted to $3.43 \pm 1.02 \times 10^{-3}\%$.

431 G. Similar to the full bimodal inference model, confidence simulated from the likelihood-
432 oscillation-only model was enhanced for stimulus-congruent choices ($\beta = 0.03 \pm 1.42 \times 10^{-4}$,

₄₃₃ $T(2.1 \times 10^6) = 191.78$, $p < 2.2 \times 10^{-308}$) and history-congruent choices ($\beta = 9.1 \times 10^{-3} \pm$

₄₃₄ 1.25×10^{-4} , $T(2.1 \times 10^6) = 72.51$, $p < 2.2 \times 10^{-308}$).

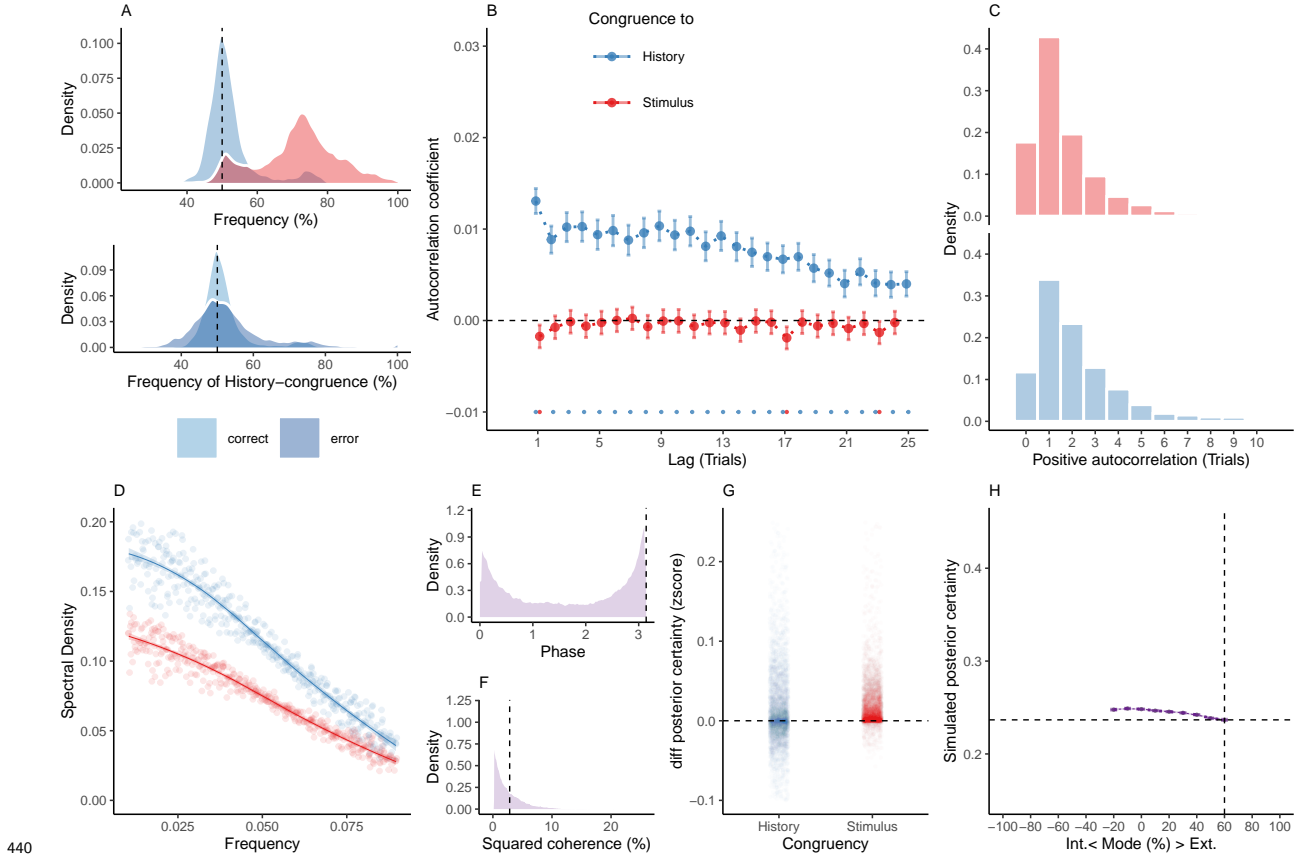
₄₃₅ H. In the likelihood-oscillation-only model, the positive quadratic relationship between the

₄₃₆ mode of perceptual processing and confidence was markedly reduced in comparison to the full

₄₃₇ model ($\beta_2 = 0.34 \pm 0.1$, $T(2.1 \times 10^6) = 3.49$, $p = 4.78 \times 10^{-4}$). The horizontal and vertical

₄₃₈ dotted lines indicate minimum posterior certainty and the associated mode, respectively.

439 **1.15 Supplemental Figure S11**



441 **Supplemental Figure S11. Reduced Control Model M3: Only oscillation of the**
 442 **prior.** When simulating data for the *prior-oscillation-only model*, we removed the oscillation
 443 from the prior term by setting the amplitude a_{LLR} to zero. Simulated data thus depended
 444 only on the participant-wise estimates for hazard rate H , amplitude a_ψ , frequency f , phase p
 445 and inverse decision temperature ζ .

446 A. Similar to the full model (Figure 1F and Figure 4), simulated perceptual choices were
 447 stimulus-congruent in $71.97\% \pm 0.17\%$ of trials (in red). History-congruent amounted to
 448 $52.1\% \pm 0.11\%$ of trials (in blue). As in the full model, the prior-oscillation-only showed a
 449 significant bias toward perceptual history $T(4.32 \times 10^3) = 18.34$, $p = 1.98 \times 10^{-72}$; upper
 450 panel). Similarly, history-congruent choices were more frequent at error trials ($T(4.31 \times 10^3)$
 451 $= 12.35$, $p = 1.88 \times 10^{-34}$; lower panel).

452 B. In the prior-oscillation-only model, we did not observe any significant positive autocor-

⁴⁵³ relation of stimulus-congruence , whereas the autocorrelation of history-congruence was
⁴⁵⁴ preserved.

⁴⁵⁵ C. In the prior-oscillation-only model, the number of consecutive trials at which true au-
⁴⁵⁶ tocorrelation coefficients exceeded the autocorrelation coefficients for randomly permuted
⁴⁵⁷ data did was decreased with respect to stimulus-congruence relative to the full model ($1.8 \pm$
⁴⁵⁸ 1.01×10^{-3} trials; $T(4.31 \times 10^3) = -6.48$, $p = 1.03 \times 10^{-10}$), but did not differ from the full
⁴⁵⁹ model with respect to history-congruence ($4.25 \pm 1.84 \times 10^{-3}$ trials; $T(4.32 \times 10^3) = 0.07$, p
⁴⁶⁰ = 0.95).

⁴⁶¹ D. In the prior-oscillation-only model, the smoothed probabilities of stimulus- and history-
⁴⁶² congruence (sliding windows of ± 5 trials) fluctuated as a scale-invariant process with a $1/f$
⁴⁶³ power law, i.e., at power densities that were inversely proportional to the frequency (power
⁴⁶⁴ $\sim 1/f^\beta$; stimulus-congruence: $\beta = -0.78 \pm 1.11 \times 10^{-3}$, $T(1.92 \times 10^5) = -706.62$, $p <$
⁴⁶⁵ 2.2×10^{-308} ; history-congruence: $\beta = -0.83 \pm 1.27 \times 10^{-3}$, $T(1.92 \times 10^5) = -651.6$, $p <$
⁴⁶⁶ 2.2×10^{-308}).

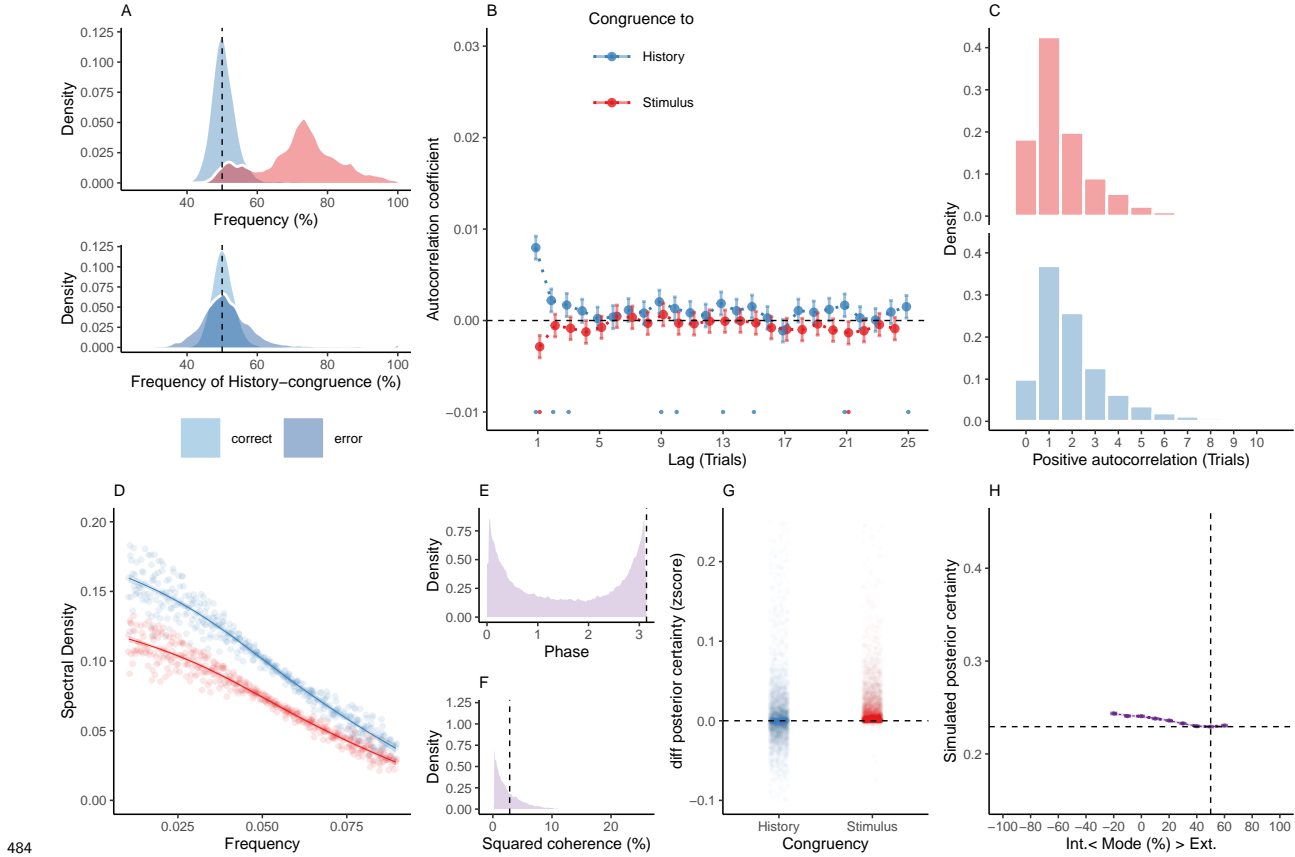
⁴⁶⁷ E. In the prior-oscillation-only model, the distribution of phase shift between fluctuations
⁴⁶⁸ in simulated stimulus- and history-congruence peaked at half a cycle (π denoted by dotted
⁴⁶⁹ line). Similar to the full model, the dynamic probabilities of simulated stimulus- and history-
⁴⁷⁰ congruence were anti-correlated ($\beta = -0.03 \pm 8.61 \times 10^{-4}$, $T(2.12 \times 10^6) = -34.03$, $p =$
⁴⁷¹ 8.17×10^{-254}).

⁴⁷² F. In the prior-oscillation-only model, the average squared coherence between fluctuations in
⁴⁷³ simulated stimulus- and history-congruence (black dotted line) was reduced in comparison to
⁴⁷⁴ the full model ($T(3.54 \times 10^3) = -3.22$, $p = 1.28 \times 10^{-3}$) and amounted to $3.52 \pm 1.04 \times 10^{-3}\%$.

⁴⁷⁵ G. Similar to the full bimodal inference model, confidence simulated from the prior-oscillation-
⁴⁷⁶ only model was enhanced for stimulus-congruent choices ($\beta = 0.02 \pm 1.44 \times 10^{-4}$, $T(2.03 \times 10^6)$
⁴⁷⁷ = 128.53, $p < 2.2 \times 10^{-308}$) and history-congruent choices ($\beta = 0.01 \pm 1.26 \times 10^{-4}$, $T(2.03 \times 10^6)$
⁴⁷⁸ = 88.24, $p < 2.2 \times 10^{-308}$).

⁴⁷⁹ H. In contrast to the full bimodal inference model, the prior-oscillation-only model did
⁴⁸⁰ not yield a positive quadratic relationship between the mode of perceptual processing and
⁴⁸¹ confidence ($\beta_2 = -0.17 \pm 0.1$, $T(2.04 \times 10^6) = -1.66$, $p = 0.1$). The horizontal and vertical
⁴⁸² dotted lines indicate minimum posterior certainty and the associated mode, respectively.

483 **1.16 Supplemental Figure S12**



484 **485 Supplemental Figure S12. Reduced Control Model M4: Normative evidence**

486 **accumulation.** When simulating data for the *normative-evidence-accumulation model*, we
 487 removed the oscillation from the likelihood and prior terms by setting the amplitudes a_{LLR}
 488 and a_ψ to zero. Simulated data thus depended only on the participant-wise estimates for
 489 hazard rate H and inverse decision temperature ζ .

490 A. Similar to the full model (Figure 1F and Figure 4), simulated perceptual choices were
 491 stimulus-congruent in $71.97\% \pm 0.17\%$ of trials (in red). History-congruent amounted to
 492 $50.73\% \pm 0.07\%$ of trials (in blue). As in the full model, the no-oscillation model showed
 493 a significant bias toward perceptual history $T(4.32 \times 10^3) = 9.94$, $p = 4.88 \times 10^{-23}$; upper
 494 panel). Similarly, history-congruent choices were more frequent at error trials ($T(4.31 \times 10^3)$
 495 $= 10.59$, $p = 7.02 \times 10^{-26}$; lower panel).

496 B. In the normative-evidence-accumulation model, we did not find significant autocor-

⁴⁹⁷ relations for stimulus-congruence. Likewise, we did not observe any autocorrelation of
⁴⁹⁸ history-congruence beyond the first three consecutive trials.

⁴⁹⁹ C. In the normative-evidence-accumulation model, the number of consecutive trials at
⁵⁰⁰ which true autocorrelation coefficients exceeded the autocorrelation coefficients for randomly
⁵⁰¹ permuted data decreased with respect to both stimulus-congruence ($1.8 \pm 1.59 \times 10^{-3}$ trials;
⁵⁰² $T(4.31 \times 10^3) = -5.21$, $p = 2 \times 10^{-7}$) and history-congruence ($2.18 \pm 5.48 \times 10^{-4}$ trials;
⁵⁰³ $T(4.32 \times 10^3) = -17.1$, $p = 1.75 \times 10^{-63}$) relative to the full model.

⁵⁰⁴ D. In the normative-evidence-accumulation model, the smoothed probabilities of stimulus-
⁵⁰⁵ and history-congruence (sliding windows of ± 5 trials) fluctuated as a scale-invariant process
⁵⁰⁶ with a $1/f$ power law, i.e., at power densities that were inversely proportional to the frequency
⁵⁰⁷ (power $\sim 1/f^\beta$; stimulus-congruence: $\beta = -0.78 \pm 1.1 \times 10^{-3}$, $T(1.92 \times 10^5) = -706.93$, $p <$
⁵⁰⁸ 2.2×10^{-308} ; history-congruence: $\beta = -0.79 \pm 1.12 \times 10^{-3}$, $T(1.92 \times 10^5) = -702.46$, $p <$
⁵⁰⁹ 2.2×10^{-308}).

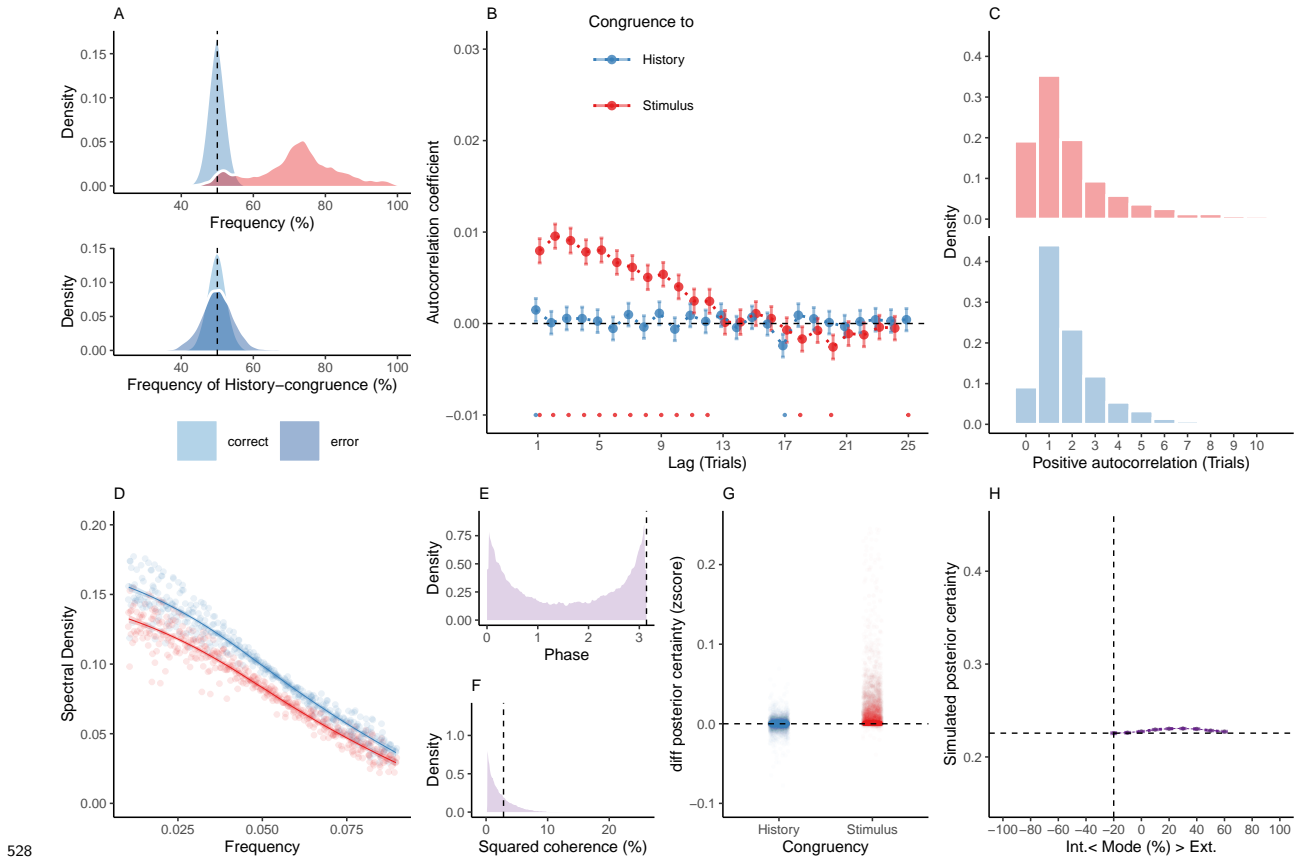
⁵¹⁰ E. In the normative-evidence-accumulation model, the distribution of phase shift between
⁵¹¹ fluctuations in simulated stimulus- and history-congruence peaked at half a cycle (π denoted
⁵¹² by dotted line). In contrast to the full model, the dynamic probabilities of simulated stimulus-
⁵¹³ and history-congruence were positively correlated ($\beta = 4.3 \times 10^{-3} \pm 7.97 \times 10^{-4}$, $T(1.98 \times 10^6)$
⁵¹⁴ $= 5.4$, $p = 6.59 \times 10^{-8}$).

⁵¹⁵ F. In the normative-evidence-accumulation model, the average squared coherence between
⁵¹⁶ fluctuations in simulated stimulus- and history-congruence (black dotted line) was reduced in
⁵¹⁷ comparison to the full model ($T(3.52 \times 10^3) = -6.27$, $p = 3.97 \times 10^{-10}$) and amounted to
⁵¹⁸ $3.26 \pm 8.88 \times 10^{-4}\%$.

⁵¹⁹ G. Similar to the full bimodal inference model, confidence simulated from the no-oscillation
⁵²⁰ model was enhanced for stimulus-congruent choices ($\beta = 0.01 \pm 1.05 \times 10^{-4}$, $T(2.1 \times 10^6)$
⁵²¹ $= 139.17$, $p < 2.2 \times 10^{-308}$) and history-congruent choices ($\beta = 8.05 \times 10^{-3} \pm 9.2 \times 10^{-5}$,
⁵²² $T(2.1 \times 10^6) = 87.54$, $p < 2.2 \times 10^{-308}$).

523 H. In the normative-evidence-accumulation model, the positive quadratic relationship between
524 the mode of perceptual processing and confidence was markedly reduced in comparison to
525 the full model ($\beta_2 = 0.14 \pm 0.07$, $T(2.1 \times 10^6) = 1.95$, $p = 0.05$). The horizontal and vertical
526 dotted lines indicate minimum posterior certainty and the associated mode, respectively.

527 **1.17 Supplemental Figure S13**



529 **Supplemental Figure S13. Reduced Control Model M5: No accumulation of**
 530 **information across trials.** When simulating data for the *no-evidence-accumulation model*,
 531 we removed the accumulation of information across trials by setting the Hazard rate H to
 532 0.5. Simulated data thus depended only on the participant-wise estimates for the amplitudes
 533 $a_{LLR/\psi}$, frequency f , phase p and inverse decision temperature ζ .

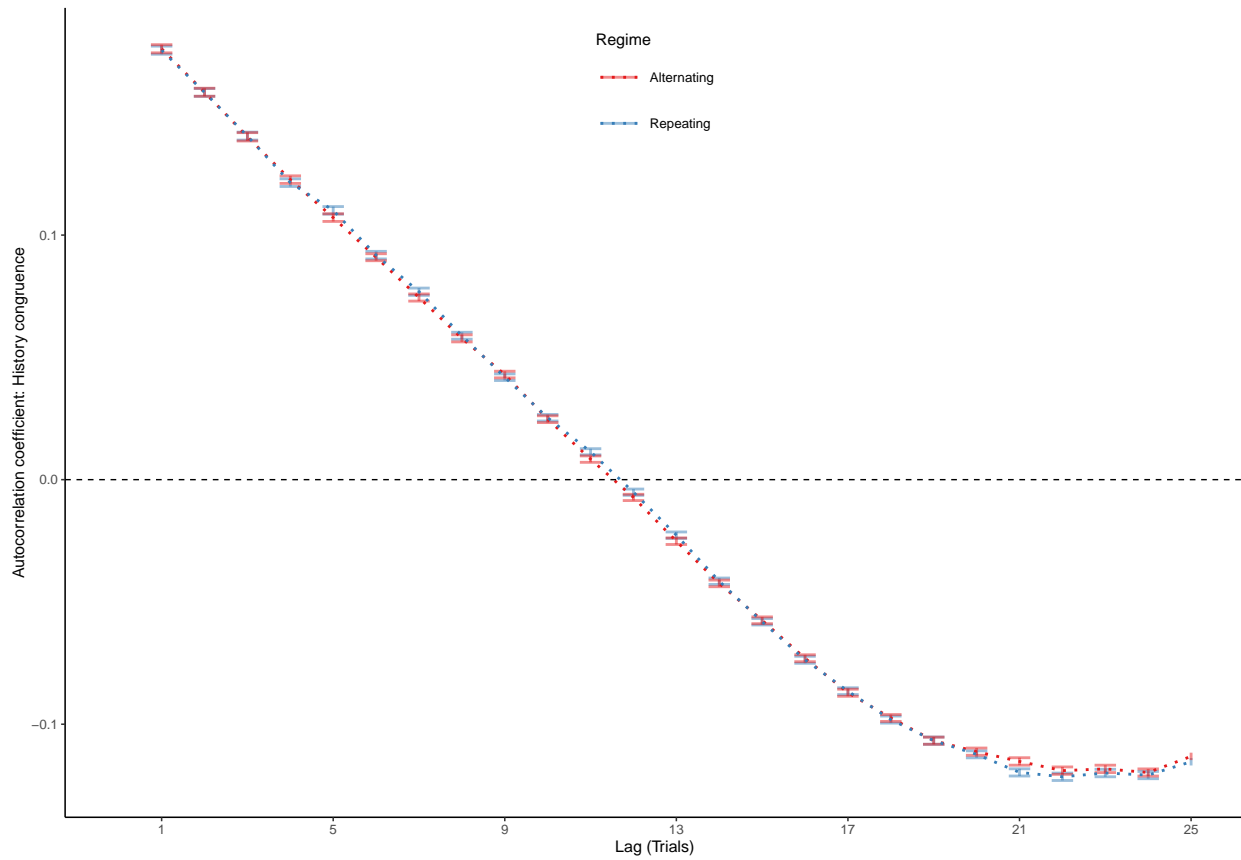
534 A. Similar to the full model (Figure 1F and Figure 4), simulated perceptual choices were
 535 stimulus-congruent in $72.14\% \pm 0.17\%$ of trials (in red). History-congruent amounted to
 536 $49.89\% \pm 0.03\%$ of trials (in blue). In contrast to the full model, the no-accumulation model
 537 showed a significant bias against perceptual history $T(4.32 \times 10^3) = -3.28$, $p = 1.06 \times 10^{-3}$;
 538 upper panel). In contrast to the full model, there was no difference in the frequency of
 539 history-congruent choices between correct and error trials ($T(4.31 \times 10^3) = 0.76$, $p = 0.44$;
 540 lower panel).

- 541 B. In the no-evidence-accumulation model, we found no significant autocorrelation of history-
542 congruence beyond the first trial, whereas the autocorrelation of stimulus-congruence was
543 preserved.
- 544 C. In the no-evidence-accumulation model, the number of consecutive trials at which true
545 autocorrelation coefficients exceeded the autocorrelation coefficients for randomly permuted
546 data increased with respect to stimulus-congruence ($2.83 \pm 1.49 \times 10^{-3}$ trials; $T(4.31 \times 10^3) =$
547 3.45 , $p = 5.73 \times 10^{-4}$) and decreased with respect to history-congruence ($1.85 \pm 3.49 \times 10^{-4}$
548 trials; $T(4.32 \times 10^3) = -19.37$, $p = 3.49 \times 10^{-80}$) relative to the full model.
- 549 D. In the no-evidence-accumulation model, the smoothed probabilities of stimulus- and
550 history-congruence (sliding windows of ± 5 trials) fluctuated as a scale-invariant process with
551 a $1/f$ power law, i.e., at power densities that were inversely proportional to the frequency
552 (power $\sim 1/f^\beta$; stimulus-congruence: $\beta = -0.82 \pm 1.2 \times 10^{-3}$, $T(1.92 \times 10^5) = -681.98$, $p <$
553 2.2×10^{-308} ; history-congruence: $\beta = -0.78 \pm 1.11 \times 10^{-3}$, $T(1.92 \times 10^5) = -706.57$, $p <$
554 2.2×10^{-308}).
- 555 E. In the no-evidence-accumulation model, the distribution of phase shift between fluctuations
556 in simulated stimulus- and history-congruence peaked at half a cycle (π denoted by dotted
557 line). In contrast to the full model, the dynamic probabilities of simulated stimulus- and
558 history-congruence were not significantly anti-correlated ($\beta = 6.39 \times 10^{-4} \pm 7.22 \times 10^{-4}$,
559 $T(8.89 \times 10^5) = 0.89$, $p = 0.38$).
- 560 F. In the no-evidence-accumulation model, the average squared coherence between fluctuations
561 in simulated stimulus- and history-congruence (black dotted line) was reduced in comparison
562 to the full model ($T(3.56 \times 10^3) = -9.96$, $p = 4.63 \times 10^{-23}$) and amounted to $2.8 \pm 7.29 \times 10^{-4}\%$.
- 563 G. Similar to the full bimodal inference model, confidence simulated from the no-evidence-
564 accumulation model was enhanced for stimulus-congruent choices ($\beta = 0.01 \pm 9.4 \times 10^{-5}$,
565 $T(2.11 \times 10^6) = 158.1$, $p < 2.2 \times 10^{-308}$). In contrast to the full bimodal inference model,
566 history-congruent choices were not characterized by enhanced confidence ($\beta = 8.78 \times 10^{-5} \pm$

₅₆₇ 8.21×10^{-5} , $T(2.11 \times 10^6) = 1.07$, $p = 0.29$).

₅₆₈ H. In the no-evidence-accumulation model, the positive quadratic relationship between the
₅₆₉ mode of perceptual processing and confidence was markedly reduced in comparison to the full
₅₇₀ model ($\beta_2 = 0.19 \pm 0.06$, $T(2.11 \times 10^6) = 3$, $p = 2.69 \times 10^{-3}$). The horizontal and vertical
₅₇₁ dotted lines indicate minimum posterior certainty and the associated mode, respectively.

572 **1.18 Supplemental Figure S14**



573
574 **Supplemental Figure S14. Autocorrelation of history-congruence of alternating**
575 **and repeating biases.** Here, we simulate the autocorrelation of history-congruence in 10^3
576 synthetic participants. In the repeating regime (blue), history-congruence fluctuated between
577 50% and 80% (blue) in interleaved blocks (10 blocks per condition with a random duration
578 between 15 and 30 trials). In the alternation regime (red), history-congruence fluctuated
579 between 50% and 20%. The resulting autocorrelation curves for history-congruence overlap,
580 indicating that our analysis is able to accommodate both repeating and alternating biases.

581 1.19 Supplemental Table T1

| Authors | Journal | Year |
|--|--|------|
| Bang, Shekhar, Rahnev | JEP:General | 2019 |
| Bang, Shekhar, Rahnev | JEP:General | 2019 |
| Calder-Travis, Charles, Bogacz, Yeung | Unpublished | NA |
| Clark & Merfeld | Journal of Neurophysiology | 2018 |
| Clark | Unpublished | NA |
| Faivre, Filevich, Solovey, Kuhn, Blanke | Journal of Neuroscience | 2018 |
| Faivre, Vuillaume, Blanke, Cleeremans | bioRxiv | 2018 |
| Filevich & Fandakova | Unplublished | NA |
| Gajdos, Fleming, Saez Garcia, Weindel, Davranche | Neuroscience of Consciousness | 2019 |
| Gherman & Philiastides | eLife | 2018 |
| Haddara & Rahnev | PsyArXiv | 2020 |
| Haddara & Rahnev | PsyArXiv | 2020 |
| Hainguerlot, Vergnaud, & de Gardelle | Scientific Reports | 2018 |
| Hainguerlot, Gajdos, Vergnaud, & de Gardelle | Unpublished | NA |
| Jachs, Blanco, Grantham-Hill, Soto | JEP:HPP | 2015 |
| Jachs, Blanco, Grantham-Hill, Soto | JEP:HPP | 2015 |
| Jachs, Blanco, Grantham-Hill, Soto | JEP:HPP | 2015 |
| Jaquiere, Yeung | Unpublished | NA |
| Kvam, Pleskac, Yu, Busemeyer | PNAS | 2015 |
| Kvam, Pleskac, Yu, Busemeyer | PNAS | 2015 |
| Kvam and Pleskac | Cognition | 2016 |
| Law, Lee | Unpublished | NA |
| Lebreton, et al. | Sci. Advances | 2018 |
| Lempert, Chen, & Fleming | PlosOne | 2015 |
| Locke*, Gaffin-Cahn*, Hosseiniaveh, Mamassian, & Landy | Attention, Perception, & Psychophysics | 2020 |
| Maniscalco, McCurdy,Odegaard, & Lau | J Neurosci | 2017 |
| Maniscalco, McCurdy,Odegaard, & Lau | J Neurosci | 2017 |
| Maniscalco, McCurdy,Odegaard, & Lau | J Neurosci | 2017 |
| Maniscalco, McCurdy,Odegaard, & Lau | J Neurosci | 2017 |
| Martin, Hsu | Unpublished | NA |
| Massoni & Roux | Journal of Mathematical Psychology | 2017 |
| Massoni | Unpublished | NA |
| Mazor, Friston & Fleming | eLife | 2020 |
| Mei, Rankine,Olafsson, Soto | bioRxiv | 2019 |
| Mei, Rankine,Olafsson, Soto | bioRxiv | 2019 |
| O'Hora, Zgonnikov, Kenny, Wong-Lin | Fechner Day proceedings | 2017 |
| O'Hora, Zgonnikov, CiChocki | Unpublished | NA |

(continued)

| Authors | Journal | Year |
|--|--|------|
| O'Hora, Zgonnikov, Neverauskaite | Unpublished | NA |
| Palser et al | Consciousness & Cognition | 2018 |
| Pereira, Faivre, Iturrate et al. | bioRxiv | 2018 |
| Prieto et al. | Submitted | NA |
| Rahnev et al | J Neurophysiol | 2013 |
| Rausch & Zehetleitner | Front Psychol | 2016 |
| Rausch et al | Attention, Perception, & Psychophysics | 2018 |
| Rausch et al | Attention, Perception, & Psychophysics | 2018 |
| Rausch, Zehetleitner, Steinhauser, & Maier | NeuroImage | 2020 |
| Recht, de Gardelle & Mamassian | Unpublished | NA |
| Reyes et al. | PlosOne | 2015 |
| Reyes et al. | Submitted | NA |
| Rouault, Seow, Gillan, Fleming | Biol. Psychiatry | 2018 |
| Rouault, Seow, Gillan, Fleming | Biol. Psychiatry | 2018 |
| Rouault, Dayan, Fleming | Nat Commun | 2019 |
| Sadeghi et al | Scientific Reports | 2017 |
| Schmidt et al. | Consc Cog | 2019 |
| Shekhar & Rahnev | J Neuroscience | 2018 |
| Shekhar & Rahnev | PsyArXiv | 2020 |
| Sherman et al | Journal of Neuroscience | 2016 |
| Sherman et al | Journal of Cognitive Neuroscience | 2016 |
| Sherman et al | Unpublished | NA |
| Sherman et al | Unpublished | NA |
| Siedlecka, Wereszczyski, Paulewicz, Wierzchon | bioRxiv | 2019 |
| Song et al | Consciousness & Cognition | 2011 |
| van Boxtel, Orchard, Tsuchiya | bioRxiv | 2019 |
| van Boxtel, Orchard, Tsuchiya | bioRxiv | 2019 |
| Wierzchon, Paulewicz, Asanowicz, Timmermans & Cleeremans | Consciousness and Cognition | 2014 |
| Wierzchon, Anzulewicz, Hobot, Paulewicz & Sackur | Consciousness and Cognition | 2019 |

⁵⁸² 1.20 Supplemental Table T2

| Parameters | Interpretation |
|------------|---|
| α | Sensitivity to sensory information |
| H | Expected probability of a switch in the cause of sensory information (Hazard) |
| a_{LLR} | Amplitude of fluctuations in likelihood precision ω_{LLR} |
| a_ψ | Amplitude of fluctuations in prior precision ω_ψ |
| f | Frequency of ω_{LLR} and ω_ψ |
| p | Phase (p for ω_{LLR} ; p + π for ω_ψ) |
| ζ | Inverse decision temperature |